7 HUMAN SCALED TUBE-CONE MODEL

7.1 Experimental methods

7.1.1 General considerations

The human tube-cone model was developed from the ovine tube-stem model. It also involved graft impaction into a tube, implant fixation and subsequent endurance testing to failure. For the human model, testing of impaction grafting procedures and graft materials was transferred from the ovine to the human dimensions. As described in the discussion section of the die-plunger compression tests (chapter 4.3), the shear-box tests (chapter 5.3) and the ovine tube-cone model (chapter 6.3), the mechanical performance of particulate aggregates is influenced by the relative ratio of particle size to cavity measurements because load transfer mechanisms and the relevance of edge effects depend on it. In the same way as with the ovine tube-stem model, the human sized tube-stem model is designed to identify correlations between the quantitative characteristics derived from the standardised tests like the die-plunger compression and the shear-box test and stability results from a more realistic, complex and clinically relevant experimental set-up like the ovine or human sized models.

Being derived from the ovine tube-stem model, the design and experimental procedure of the human tube-cone model was also derived from the graft preparation steps, the femur-stem geometry, loading regime and failure modes in clinical impaction grafting. At the same time it provided a sufficiently high abstraction level of the test geometry, sample preparation, impaction procedure, loading regime and test criteria to control or keep constant process variables in favour of reproducibility and thus isolate the desired parameters as the major variables of the test. In the case of the human tube-cone model the parameter focus was expanded from the graft mixing ratios of the ovine model to a much wider range of bone grafts, synthetic extenders and bone/ceramic mixing ratios. An overlap of identical graft configurations between the ovine and human sized model was included in the experimental plan to allow a comparison between both models. Besides a wider range of graft materials the human model was expanded by a new design and procedure named the “Impactometer” to replicate and control impaction levels, a factor considered as highly critical for clinical success but relying on subjective manual feedback not controlled in surgical practice.

The human tube-cone model incorporated some additional design simplifications or process abstractions over the ovine model in order to further reduce the influence of methodological variables which are difficult to control or to make the experiments more efficient with regards to time, cost and safety. These measures were waiving cementation, using a rotationally symmetric cone instead of a double-tapered polished stem and limiting the cyclic loading to the vertical axisymmetric direction only.

Cementation was omitted for the human tube-cone model because a proportion of the clinical impaction grafting procedures are performed cementless and cementation seemed of limited relevance when the investigation focused on graft materials and impaction levels as the major process variables to be isolated. From the results of the ovine model it was seen that critical subsidence was caused within the graft and not the cement and that the cement-graft interface was relatively weak with low cement penetration into the graft. Therefore the exclusion of cementation seemed a scientifically valid measure to improve experimental reproducibility and isolation of the critical factors to be investigated. At the same time leaving out cementation made the procedure more time efficient, less user dependent, cheaper and safer.

The use of a polished double-tapered hip stem in the ovine model was mainly the consequence of using cement for stem fixation where surface finish and taper are essential for secure long term fixation. In addition, as the ovine model was also developed for ethical approval of an animal study in sheep, close similarity between clinical and experimental impaction grafting seemed necessary. Without both conditions, cement and animal study preparation, the use of a double-tapered polished stem for the human model experiments seemed less binding and a non-polished metal cone more justified. The cement mantle also changes the geometry and dimensions in contact with the impacted bone graft by rounding off the edges created by the double-taper and by increasing the circumference. With the cement, the surface in contact with the graft is also not polished but it is the rougher exterior of the cement mantle. Considering this, the stem plus cement forms a cone-like object supported by impacted graft so that the use of a non-polished metal cone seemed valid. The metal cone should guarantee a comparable load transfer into the graft and analogous load pattern in the graft mantle as the cemented stem. Furthermore, as the human model was loaded in vertical axisymmetric compression only, the stability against torsion or bending that might be provided by a non-rotationally symmetric cross-section of a double-tapered stem did not matter. The sharper profile, smoother surface and slightly smaller dimensions of the metal

cone versus the stem-plus-cement combination is expected to, if anything, increase loading of the graft and accelerate subsidence.

The limitation to vertical loading axisymmetric with the metal cone is a valid abstraction considering that massive vertical subsidence is the major failure mode during the post-operative phase where initial stability is crucial. Torsional stability in impaction grafting is expected to be dominated by the stem cross-section and profile and much less influenced by the graft material or impaction levels, the two factors to be investigated in this study. By using a cone with a circular cross-section as a model for the stem, the experiment deliberately excluded stem shape as an influential factor.

7.1.2 Design tube-cone model

The geometry of the human tube-cone model was designed to reproducibly expose the graft to a stress pattern comparable to that experienced *in-vivo*. An experienced surgeon performed an impaction grafting procedure using a cemented hip stem in a Sawbone glass fibre femur which was sectioned post-operatively in equidistant segments of 10mm height (figure 7.1).

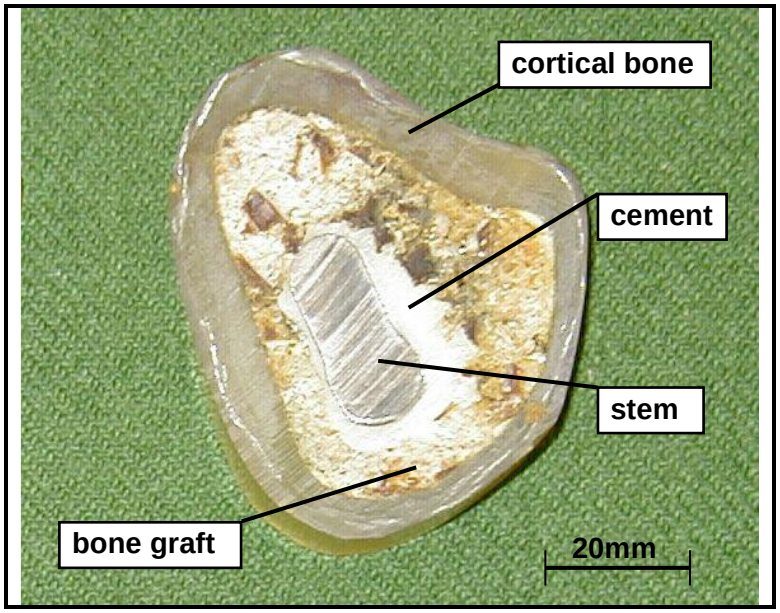

Figure 7.1:
Proximal cross-section of a Sawbone femur showing a cemented impaction grafting.

The morphology of the medullary canal was found distally to resemble a cylindrical tube which widened conically towards the proximal end. The cross-sections were planimetrically analysed to derive a mean surface equivalent femoral diameter for the tube and to correlate

the cross-sectional surface area of the double-tapered stem to the proximal diameter and taper angle of a cone. This way a diameter ratio between tube and cone was ensured which was comparable to that between the medullary canal and the cemented stem of a clinically impaction grafted hip. The cone length was equal to the typical stem length used in impaction grafting and the length of the tube was chosen so that the inserted cone resembled a depth of graft commonly found clinically between the most distal part of the stem and the distal plug. Figure 7.2 is taken from the Howmedica surgical instruction manual and shows a surgical stem alignment template superimposed onto an x-ray image of a typical hip to be revised by impaction grafting. The shapes, positions and dimensions of femur, distal plug, stem and cement to be modelled by the human tube-cone set-up are clearly visible and compare well to the dimensions chosen in the experimental model shown in figure 7.3. This way bone graft can reproducibly be exposed to a stress pattern comparable to that *in-vivo*.

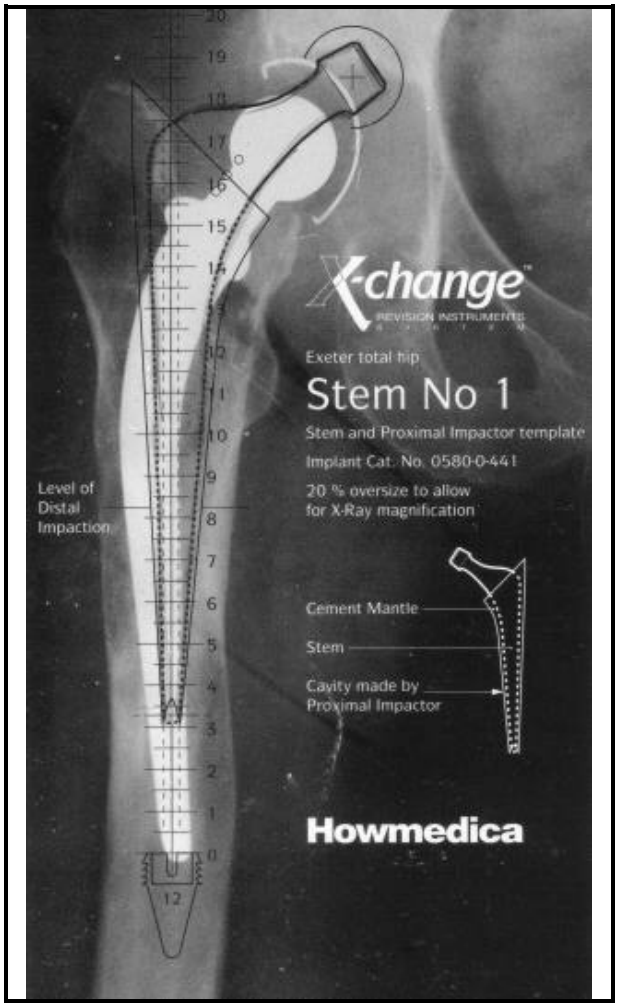

Figure 7.2:
Surgical stem alignment template superimposed onto an x-ray image of a typical hip to be revised by impaction grafting [41].

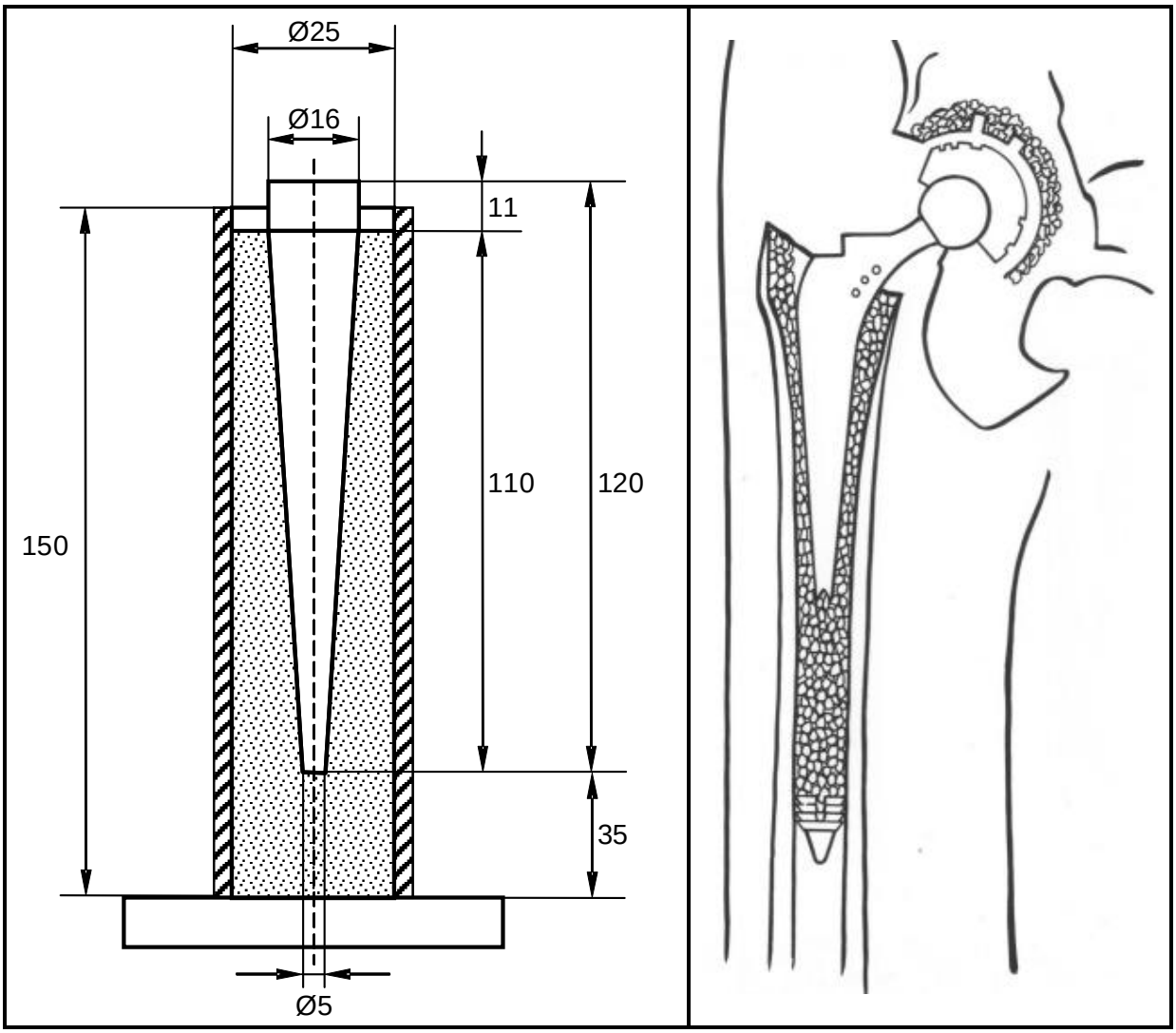

Figure 7.3: *Comparison between a sketch of the human size tube-cone model (left) and a drawing from the surgical instruction manual showing the trial reduction (right)* [41].

From the analysis of the Sawbone cross-sections and the surgical instructions a steel tube with a diameter of 25mm and a length of 150mm was derived. As with the ovine model, the slightly conical proximal cross-section was not modelled to improve experimental reproducibility by reducing variables of the impaction process. A cylindrical canal made it possible to limit the distal impactor sizes to one allowing the simple control of graft charges and impaction energy and forces delivered into the graft. A wall thickness of 4mm made the steel tube so stiff, that effects from the variable elasticity or strength of the femoral bone *in-vivo* were excluded for improved reproducibility and parameter isolation. The superior stiffness of a solid tube over a femoral bone could result in graft stresses higher *in-vitro* than *in-vivo*, potentially accelerating failure. This was considered a tolerable or favourable effect because the model was designed for a relative stability comparison between graft materials or impaction energies and it was accepted that absolute numbers from any *in-vitro* impaction grafting test cannot be compared to the *in-vivo* reference unscaled.

The cone mimicked the stem geometry with a total length of 120mm comprising a conical section of 110mm length with the diameter increasing from 5mm distally to 16mm proximally as shown in figure 7.3. At the proximal end the cone extended with a cylindrical section of 10mm length. During impaction the cone was inserted into the compacted graft up to separating line between the conical and cylindrical section (figure 7.3). This way it was ensured that a subsiding cone did not wedge deeper into the graft than at the zero position. The cone had a central bore hole of 3.6mm diameter to be aligned with and allow low friction movement along a guide wire. The guide wire was taken from the surgical Howmedica tool kit and had a diameter of 3.5mm. The surface finish of both the tube and the cone was smooth from machining and sanding but not polished. Intense washing and frequent sanding with fine paper ensured that the surface finish remained constantly smooth throughout the test period. Figure 7.4 shows a photo of the tube and cone of the human model.

Figure 7.4:
Tube and cone of the human size impaction grafting model.

At the distal end of the tube a ring was welded on as an adapter to bolt the tube onto a circular plate as seen in figure 7.3. The end plate acted like a distal plug closing the tube distally and offering a central thread to hold the guide wire. The plate could be removed for easy cleaning and acted as an adapter for mounting the human model first into the impaction device and finally into the test machine. Cone length, the depth of the distally closed tube and cone insertion to the separating line between the conical and cylindrical section ensured that the distance between the distal ends of cone and tube measured 35mm, a value lying in the clinically recommended range.

7.1.3 Design impactometer

When graft impaction is performed manually as in surgery or in the ovine tube-stem model the impaction energies and forces cannot be monitored or controlled although impaction quality is seen as a major factor crucial for clinical success. In clinical impaction grafting the surgeon has to balance the requirement of intense impaction with the risk of femoral fracture and must rely on his strength and experience. During manual impaction as a part of the ovine model procedure, impaction was as vigorous and intense as possible because a risk of fracture did not exist. However, this method did not allow controllable impaction.

In order to standardise, monitor and control impaction energy and forces in the model the impactometer was designed. As shown in a design sketch (figure 7.5), the Impactometer was a simple device consisting of a constant mass which could be dropped from various heights along the guide wire to allow hammer blows of controllable energy and momentum. With a hammer mass of m= 612g and a drop height variable from h= 0-600mm, the energy and momentum per individual hammer blow could be adjusted from zero to 3.6J or 2.1Ns respectively. The drop height could be held constant between blows either by an adjustable cable between mass and cone or by a height adjustable clamp on the guide wire including a pointer for a ruler attached to the tower. The solid tower allowed support and tensioning of the thin guide wire as well as the easy removal of the weight, tube-cone model and wire when the impaction process was finished. Figure 7.6 shows a photo of the assembled impactometer.

The cone was connected to a LVDT position transducer which recorded the set per hammer blow, the distance the cone or the distal impactor travelled per individual hammer blow or in accumulation. The distal impactor was formed by a removable flat metal disk clipped onto the distal end of the cone. This way a two stage impaction could be replicated from the clinical situation where a distal impactor compresses the graft vertically and a proximal impactor with the shape of an oversized prosthesis also compresses the graft radially. The transducer allowed a resolution of 0.01mm and thus was more sensitive to impactor displacement as a form of feedback from the impaction process than during manual impaction grafting.

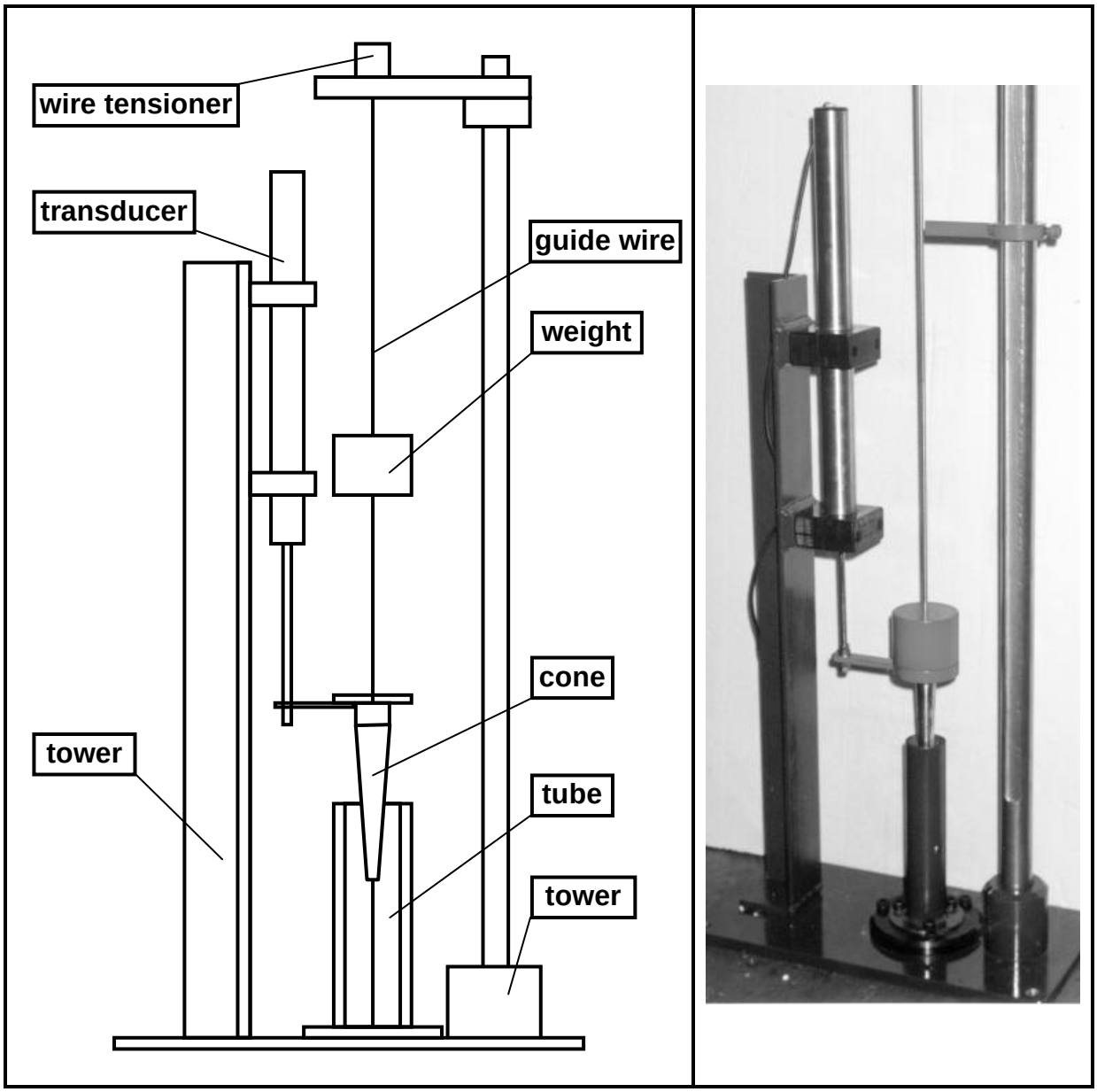

Figure 7.5: *Design sketch (left) and photo of the impactometer used for the controlled delivery of impaction energy and momentum.*

7.1.4 Design test procedure

The test procedure consisted of two parts, firstly the controlled graft impaction using the impactometer and secondly the cyclic block loading of the human tube-cone model until failure. The impaction procedure was modelled on the clinical practice where initially the medullary canal is filled with individual charges of graft which are then compacted axially with flat distal impactors by a individual sets of hammer blows. Thereafter the proximal impactors resembling the shape of the hip stem are used to compact the graft further both vertically and radially thus creating a cavity for stem insertion. Also with the tube-cone model

mounted into the impactometer a distal impactor was used to axially compact individual charges of measured graft volumes first with defined impaction energies delivered by specific numbers of hammer blows constant for a chosen impaction level. After this pre-compaction, the cone was impacted into the filled graft tube with hammer blows from the same consistent drop height as during pre-compaction. This way the graft was compressed further both axially and radially as during clinical impaction grafting.

Depending on the impaction level chosen and thus the total graft quantity required to fill the tube, specific graft volumes ranging from $30cm^3$ to $50cm^3$ were measured using small cup-like containers like shown in figure 7.6 and charged into the tube using a funnel to ensure homogenous distribution of the graft phases. During the preparation of the graft volumes and during charging them into the tube it was important to avoid segregation of graft phases and particle sizes by proper mixing and container tapping. Volume mixing and charging as described was preferred to potentially more accurate weight charging as it was expected to become the preferred clinical method when bone graft plus extender mixes must be produced in the operating theatre and ease of handling and sterilisation matters.

Figure 7.6:
Preparation of constant graft volumes for controlled charging and impaction with the human tube-cone model by using cup-like containers. The container shown holds a $30cm^3$ volume of a 2:1 bone/ceramic graft mix.

Depending on the impaction level chosen for an individual test, a specific number of hammer blows from a constant drop height was exerted onto the distal impactor and compressed a graft charge before the next one was added and the process repeated until the tube was filled with graft compacted up to a line 5mm below the proximal end of the tube. The position of the impactor between graft charges and the set per hammer blow were documented.

The standard drop height was set at 260mm to deliver the same momentum on impact as calculated from intra-operative measurements where the hammer weight, sliding distance and hammer frequency resulted in an average hammer momentum of ca. 1.4Ns, a value close to the 1.2Ns momentum claimed from a non-disclosed method of intra-operative measurement in the literature[23.4x]. The energy delivered per hammer blow from the 260mm standard drop height equated to 1.55J. The total impaction intensity delivered during pre-compaction was given as the accumulated energy from all pre-compaction hammer blows. The pre-compaction energies tested with the human tube-cone model ranged from 3.1J to 23.3J with 6.2J as the standard pre-compaction energy. The pre-compaction energy correlated with the total impaction energy and was used to identify the impaction levels tested. Hammer drop height was varied from 130mm to 520mm to investigate how hammer momentum and thus peak force affect stability when the total compaction energy is kept constant.

After graft charging and distal compaction was completed the flat disk was removed from the distal end of the cone so that it could be impacted into the graft filled tube by repeated hammer blows from the same drop height as during the pre-compaction phase. The set per hammer blow was measured and cone impaction was stopped when 6mm of the cylindrical proximal end of the cone protruded from top of the tube. This constant position ensured that the conical section of the cone was always fully impacted into the bone graft.

With a tube volume of 73.6cm^3 resulting in a 71.2cm^3 graft column by limiting charging and compaction to a line 5mm below the proximal end of the tube and with an inserted cone volume of 41.6cm^3, the condensed graft volume measured 29.6cm^3. Depending on the pre-compaction energy delivered, the original graft volume charged into the tube varied between ca. 90cm^3 and 120cm^3 and thus resulted in a total graft compaction ratio of ca. 3.0 to 4.1 or equivalent average compression strains of ca. 0.67 to 0.76. A rough estimation of peak forces required to achieve such compression ratios can be based on the stress-strain relationships established under quasi-static compression as performed during die-plunger testing. This comparison indicates hammer peak forces exceeding several 1000N.

When pre-compaction and cone impaction were completed, the guide wire was removed and the graft filled tube with the inserted cone was disconnected from the impactometer. Then the tube-cone model was mounted into an Instron 8511 servo-hydraulic testing machine for cyclic block loading as shown in figure 7.7. The loading regime was similar to the ovine tube-stem tests but the vertical compression load was applied only co-axially with the cone and the peak loads of the successive blocks were increased from the initial 0.2kN in 200N steps until

failure at a total accumulated subsidence of 6mm. This level of subsidence was the geometrical maximum of the model design and correlates with clinical failure scenarios where such displacement can result in misalignment and malfunction of the joint and thus cause pain requiring revision. Consistent with the ovine model each load block consisted of 5000 haversine cycles run at a frequency of 2Hz. The haversine wave form was chosen because with its non-continuous signal curve it more closely imitates the steep loading gradients of human gait than a smooth sine signal. The cycling frequency was chosen to lie in the bandwidth of human walking speeds so that the graft response is affected by the same viscoelastic properties experienced *in-vivo*. Vertical subsidence as the major failure mode in clinical impaction grafting was recorded permanently by applying an averaging algorithm on the position signal acquired from the position transducer of the actuator using Hewlett-Packard DT-Vee software. After test completion at 6mm total subsidence the cone was removed from the grafted tube by applying a torque, for which the peak value was recorded.

Figure 7.7:
Human tube-cone model after graft impaction and cone insertion mounted into Instron 8511 servo-hydraulic testing machine for cyclic block loading..

As with the ovine model, it was accepted that the experimental design with its abstracted geometry, simplified procedure and loading regime does not allow direct quantitative comparison of numerical data with subsidence measured *in-vivo*. However only with this compromise did it became possible to constantly reproduce and control test conditions and to isolate the desired parameters graft material and impaction quality as the only variables. The impaction quality was varied by altering impaction energies with a constant hammer momentum and by altering the hammer momentum or force while keeping the total impaction energy constant. The impaction energy was varied by altering the pre-compaction energies from 3.1J (low), 6.2J (standard), 9.3J (high) to 23.3J (very high). The hammer momentum was varied from the standard 1.4Ns (drop height h=260mm) to 1.0Ns (h=130mm) and 2.0Ns (h=520mm). A summary of the experimental design, procedures and variables is given below:

Design tube-cone model

tube:	length	l_{tube}= 150mm		
	diameter	d_{tube}= 25mm		
cone:	***conical section***		***cylindrical section***	
	distal diameter	d_1= 5mm	diameter	d_3= 16mm
	proximal diameter	d_2= 16mm		
	length	l_{cone}=110mm	length	l_3=11mm

Design impactometer

guide wire:	diameter	d_w= 3.6mm
	length	l_w=1000mm
hammer:	mass	m= 612g
transducer:	resolution	0.01mm

Block loading regime

wave form: haversine
frequency: f= 2Hz
peak load: F_{max}=0.2kN to 2.6kN in 0.2kN load steps
block duration: 5000 cycles
failure criterion: 6mm subsidence

Test Procedure

1. ***Mounting*** tube-cone model in impactometer
2. ***Mixing*** of graft phases
3. ***Graft charging*** in constant volumes V= 30cm^3 to 50cm^3
4. ***Graft pre-compaction*** with distal impactors
   Multi-stage graft charging and pre-compaction with sets of hammer blows
   standard drop height h= 260mm equivalent to 1.4Ns momentum and 1.55J energy
5. ***Cone impaction*** with successive hammer blows until inserted to cylindrical section
6. ***Removal*** of guide wire and dismounting tube-cone model from impactometer
7. ***Mounting*** tube-cone model in Instron 8511 servo-hydraulic test machine
8. ***Block loading*** to failure (6mm subsidence)
9. ***Torque release*** *of the cone*

Test variables

graft materials	see section 7.2	
impaction energy	pre-compaction energy (constant hammer momentum	3.1J, 6.2J (standard), 9.3J, 23.3J p= 1.4Ns)
impaction momentum	hammer momentum (constant pre-compaction energy	0.7Ns, 1.0Ns 1.4Ns (standard), 2.0Ns 6.2J)

7.2 Materials

The graft materials tested for stability with the human tube-cone model were human bone graft as the gold standard in impaction grafting, formalin fixed ovine bone graft as an *in-vitro*

experimental graft material and various graft mixes comprising ovine bone and granules of a synthetic ceramic bone graft extender in various mixing ratios and ceramic configurations. Bone plus ceramic volumetric mixing ratios were varied from 2:1 bone/ceramic to 1:1 and 1:2 bone/ceramic. The ceramic configuration was varied with regards to particle size, sintering temperatures, porosity level and chemical composition.

When such material or impaction parameters were varied in the tests, only one variable was changed at a time while the other conditions or parameters remained constant. Therefore the experimental variables formed a multi-dimensional co-ordinate system with a standard configuration for graft material and impaction level as the origin and co-ordinate axes along which parameters were varied. This standard configuration was a 1:1 volume mix of ovine bone with a ceramic graft extender comprising granules of 2-4mm particle size sintered at T_{sint}=1150°C from an 80:20 HA/TCP composite with 25% porosity level. This specific standard configuration was chosen because an equally weighted bone/extender mix with a ceramic composition dominated by bone mineral like HA was expected to become the bone/extender composition most likely to be used clinically. As mentioned before in chapter 7.1.4, the standard impaction level chosen was the 6.2J pre-compaction energy delivered by hammer blows from a 260mm drop height resulting in a momentum of 1.4Ns.

In correlation with the ceramic variables analysed during the die-plunger tests, the granule size of the ceramic was varied between small (1-2mm), medium (2-4mm, standard) and large (4-6.3mm). The porosity levels investigated were no porosity (0%), medium porosity (25%, standard) and high porosity (50%) and the sintering temperatures changed between 1050°C (low), 1150°C (standard medium) and 1200°C (high). A reverse chemical composition of the ceramic (20:80 HA/TCP) was tested as well as one additional completely different ceramic extender from another manufacturer (pure HA, 68% porosity, 2-5mm particle size).

As during the previously described tests the preparation of bone grafts and the mixing with the ceramic extender was undertaken with large volumes at a time in order to level out variability and to ensure homogenous mixing. A minimum of three tests per parameter configuration were performed to derive an average stability performance. For pure ovine bone and for the standard 1:1 bone/ceramic mix six tests were conducted. Figure 7.8 shows photos of ovine bone and the HA/TCP ceramic in pure form prior to mixing and compares them to images of the three tested mixing ratios. A summary of the material configurations tested with the human tube-cone model is given below:

Graft materials

pure human bone	irradiated at 2.5MRad, Norwich bone mill
pure ovine bone	formalin fixed, Norwich bone mill
graft mixes	bone plus ceramic extender volume ratios: 2:1, 1:1, 1:2
pure ceramic	standard configuration: 80:20 HA/TCP, 25% porosity, 2-4mm particle size, T_{sint}= 1150°C

Ceramic parameters varied in 1:1 bone/ceramic mix

porosity:	0%, 25%, 50%
sintering temperature:	1050°C, 1150°C, 1200°C
particle size:	1-2mm, 2-4mm, 4-6.3mm
chemical composition:	80:20 HA/TCP, 20:80HA/TCP
extra material:	pure HA, 68% porosity, 2-5mm particle size

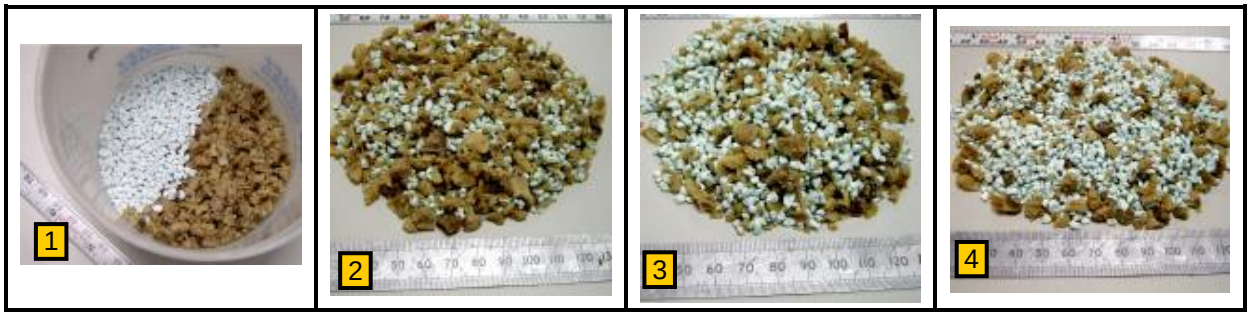

Figure 7.8: *Pure ovine bone and the standard ceramic prior to mixing (1), 2:1 bone/ceramic mix (2), the standard 1:1 mix (3) and the 1:2 bone/ceramic mix (4).*

7.3 Results

7.3.1 Endurance testing

Cones as stem models were impacted into pre-compacted graft and then cyclically block loaded in vertical compression while vertical subsidence was recorded. The qualitative relationship between number of cycles or load blocks and the subsidence was fundamentally the same for all samples, for all bone graft materials and for all load blocks tested and thus similar to the qualitative subsidence behaviour observed using the ovine model (chapter 6). As can be seen in figure 7.9 for a wide range of materials and impaction energy levels, cyclic loading initially caused steep subsidence during the first cycles before the subsidence rate declined and finally entered a state of permanent subsidence with a logarithmically decreasing gradient. This behaviour is qualitatively identical with observations made in a study on implant stability in impaction grafted human cadaveric femurs[227]. The gradient of the logarithmic function varied between load blocks and different materials. During the recovery time between individual load blocks a small fraction of the subsidence was recovered by

elastic recoil. A characteristic pattern of all materials and samples was that the subsidence per load block increased with the rising peak load of the load block.

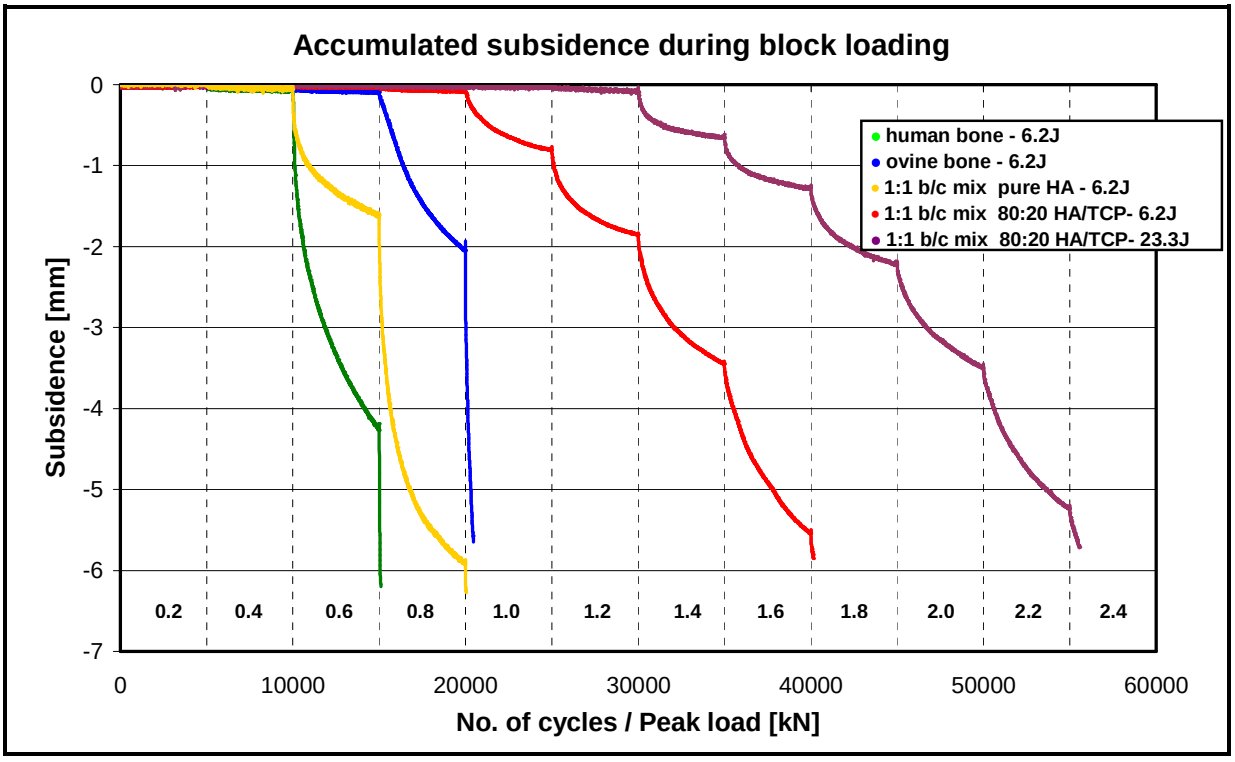

Figure 7.9: *Accumulated subsidence during cyclic block loading of a large range of typical samples of different graft materials and impaction energy levels.*

Figure 7.9 shows that different graft materials and different impaction levels had an enormous effect on initial stability. Only a block load experiment was able to resolve such a wide range of results. The least stable sample, a cone impacted into pure human bone graft pre-compacted with the standard 6.2J energy, failed during the 0.8kN load block after just slightly more than 15,000 cycles while a sample with a 1:1 bone/ceramic graft mix of identical impaction quality survived until the completion of more than 40,000 cycles during the 1.8kN load block. When such a graft mix was highly pre-compacted using 23.3J as the highest pre-compaction energy tested, failure only occurred when the peak load reached 2.4kN and more than 56,000 cycles were completed. Despite these huge stability differences, the qualitative relationship between number of cycles and subsidence remained identical for all samples. During the first load blocks, all materials appeared highly stable with small amounts of subsidence accumulating. However, depending on graft material and pre-compaction energy, significant subsidence started to accumulate when a certain peak load was exceeded. The subsidence rates soon approached a logarithmic relationship between number of cycles and subsidence. Differences between materials, levels of impaction energy and even load blocks are expressed just by skewing and shifting this functional relationship towards different subsidence rates and the number of cycles it takes to approximate this relationship.

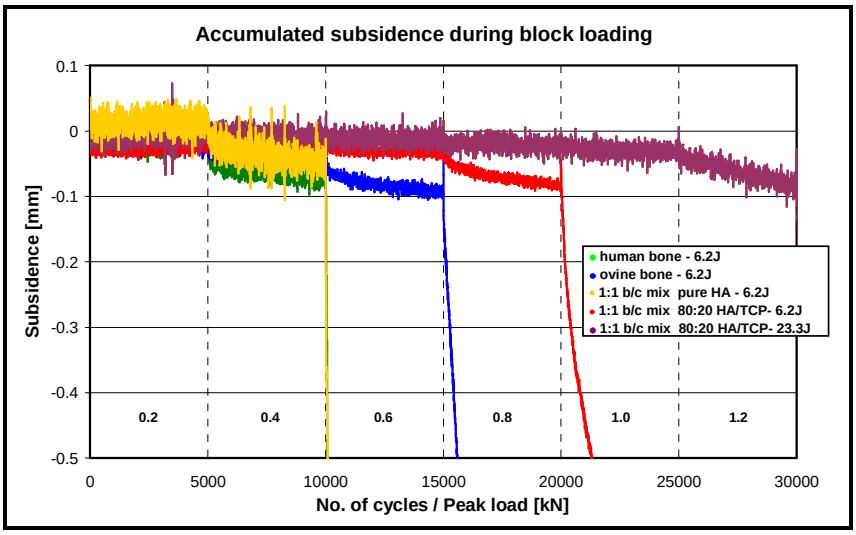

Figure 7.10:
Accumulated stem subsidence during block loading of a large range of typical samples of different graft materials and impaction energy levels (magnified chart section).

Figure 7.10 represents a magnified section of figure 7.9 with the subsidence axis limited to a total displacement of only -0.5mm. It shows that even during the high stability phases observed for the initial load blocks small amounts of subsidence measuring less than 100µm accumulated. However, even those allowed the differentiation of finally distinctive stability levels at very early stages of the block loading regime. Figure 7.11 also shows a magnified section of a subsidence chart with the subsidence curves of individual load blocks starting at 0 each and with an even higher zoom factor. The material tested was a very stable 1:1 bone/extender mix with a non-porous ceramic (0% porosity) and it can be seen that apart from a very small amount of initial subsidence during the first ca. 200 cycles measuring ca. 1-3µm no further subsidence occurred during the first three load blocks. Only the fourth 0.8kN load block exposed a clear logarithmic subsidence behaviour again. The scattered profile of the subsidence curves is the result of the resolution of the displacement transducer and the tolerance inherent in the position averaging algorithm employed. As can be seen in figures 7.10 and 7.11, the error tolerance of the signal had an approximate maximum of ± 5µm.

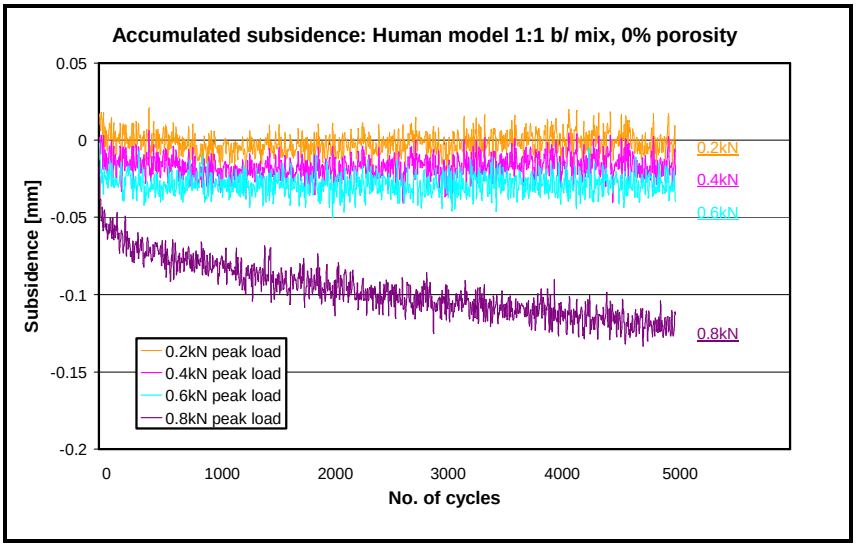

Figure 7.11:
Accumulated stem subsidence during block loading of a highly stable 1:1 bone/extender graft mix containing non-porous ceramic granules (magnified chart section).

The subsidence behaviour during load blocks of higher peak force hence, greater cone displacements, is highlighted in figure 7.12 for a 1:1 bone/ceramic graft mix, pre-compacted with 23.3J, the highest pre-compaction energy level tested. Against a logarithmic axis for number of cycles all subsidence curves asymptotically approached linear trendlines. Therefore the functional relationship between subsidence and number of cycles approximated to a logarithmic correlation with a constant subsidence rate α according to equation 7.1. Such behaviour was observed for all graft materials, impaction energies, stability levels and all peak loads where subsidence was high enough to exceeded ca. 0.1mm. The higher the subsidence rate α at a specific load the earlier failure was reached at 6mm displacement and the less mechanically stable a sample was. When the peak force was increased the subsidence rate also increased and in the sample of figure 7.12 it grew from 12µm/ln*N* during the 1.2kN load block to 659µm/ln*N* during the penultimate load block with 2.2kN peak force.

As can be seen in figure 7.12, the equilibrium of a constant subsidence rate α was reached after different numbers of cycles altering between ca. 10 to 1000. Then the correlation coefficient R^2 between subsidence curve and logarithmic trendline was greater than 0.99 and only dropped lower when signal tolerance and subsidence were of similar magnitude. Then, approximation accuracy was affected as can be seen for subsidence during the 1.2kN load block. The number of cycles required for the subsidence curve to approximate the logarithmic trendline was lower for low peak forces and higher for higher peak forces. However, as can be seen in figure 7.12 for one of the longest lasting samples, even at extreme stability levels and thus very high peak forces logarithmic subsidence with a constant subsidence rate α was finally reached. Different graft materials impaction levels and peak forces of a load blocks only tilted (subsidence rate α), shifted (vertical position constant c) or skewed (constant b) the functional equation as expressed by the parameters of equation 7.2.

$$s = -\alpha * \ln(N) - c \qquad \textit{(equ. 7.1)}$$

$$s = -\alpha * \ln(N + b) - c^* \qquad \textit{(equ. 7.2)}$$

s= accumulated subsidence [s]= mm
α = subsidence rate, [α]= $\mu m/\ln N$
N= number of cycles into load block
c= vertical start position [c]= mm
b= skewing constant
c*= vertical position constant [c*]= mm

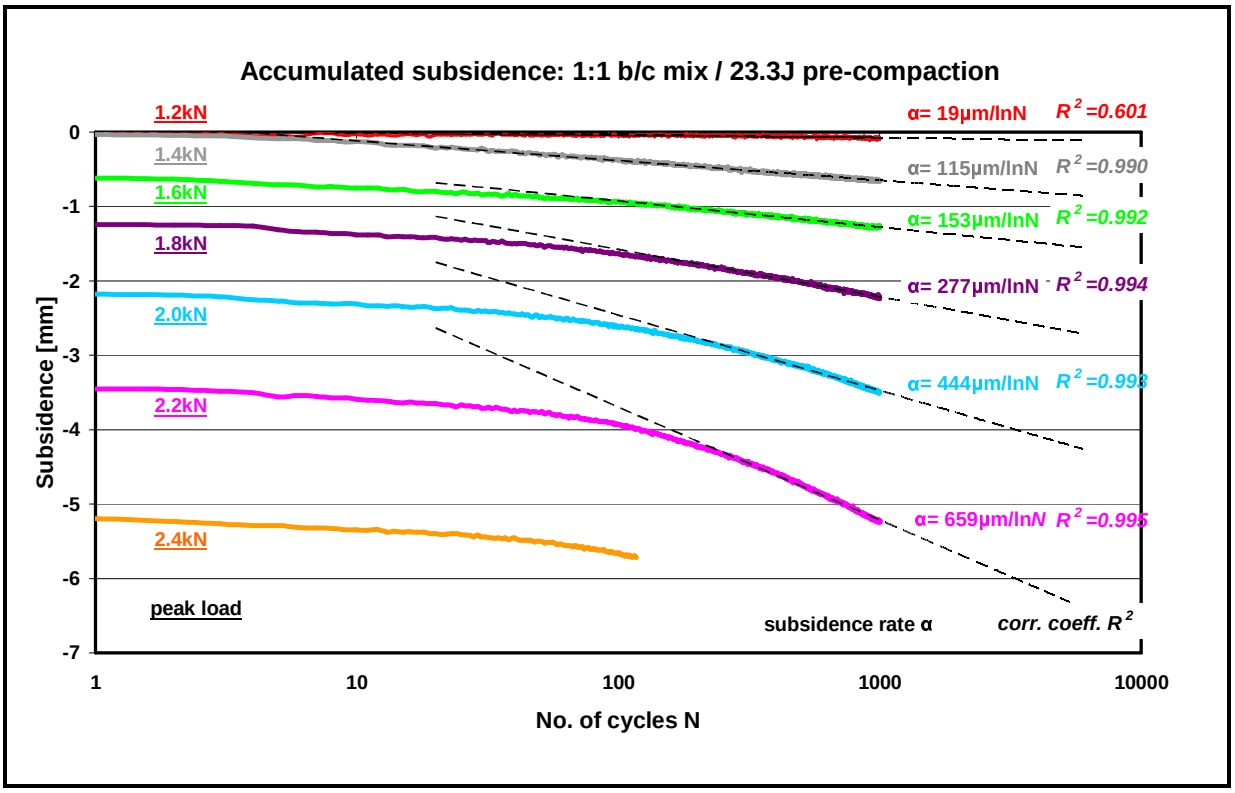

Figure 7.12: *Accumulated subsidence during cyclic block loading for exemplary samples of pure ovine bone and to bone/ceramic mixes with volume ratios of 1:1 and 1:9 bone/ceramic.*

Most qualitative characteristics of cone subsidence in the human tube-cone model are the same as observed for the ovine tube-stem model. The significant differences are highlighted in figure 7.13 where subsidence curves from the ovine and the human model are compared to each other for two samples of pure fixed ovine bone as an identical graft material. In the ovine model subsidence during each load block showed very steep initial subsidence but then the gradient rapidly decreased to follow a logarithmically constant subsidence rate. In the human model subsidence during each load block initially was less steep but the gradient took longer to decrease and follow a logarithmic relationship with the number of cycles. In the ovine model significant elastic recovery was measured after the completion of a load cycle whereas when the human model was used, elastic recovery was much smaller so that the resolution of the chart hardly can represent it. In both models the subsidence per load block and the subsidence rate increased from one load block to the next. Tests with the human model showed relatively high stability with low subsidence and small subsidence rates during the first load blocks and very high subsidence with great subsidence rates during the final load blocks leading to failure at 6mm vertical displacement. However with the ovine model, significant subsidence was observed already during the first low force load blocks but the increase in subsidence accumulation and rate was less steep than with the human model. As in the case represented in figure 7.13 and in several other samples tested with the ovine model, the subsidence rate during the final load block decreased again when vertical displacement

approached the failure criterion and the geometrical limit of the set-up. This behaviour was not observed when the human model was used. Finally, with both models the samples charged with identical bone grafts impacted either vigorously by hand or in a controlled manner using the impactometer failed during the same load block and after a comparable number of cycles.

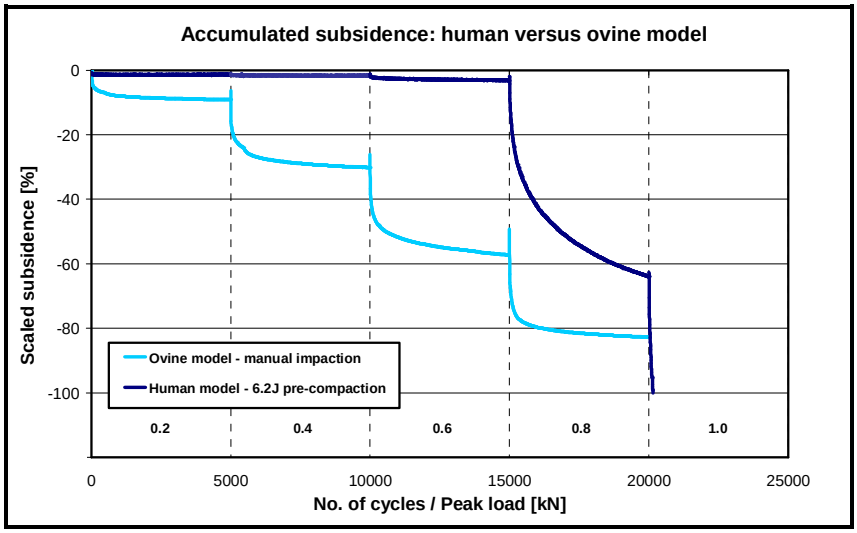

Figure 7.13:
Comparison of stem subsidence during block loading of ovine bone graft tested with the ovine model (light blue) and the human model (dark blue).

The calculation of subsidence rates for all samples and load blocks is a very time consuming procedure producing enormous quantities of data which cannot be analysed efficiently. The large bandwidth of graft materials and impaction conditions resulted in such a wide range of failure points that subsidence rates for specific load blocks could not be compared. Testing with the ovine model and the described validation with the human model above established a direct correlation between graft stability on the one hand and both subsidence rates or number of cycles to failure on the other, so that the number of cycles to failure can be used equivalently to identify and comparatively quantify graft stability. Also established was the fact that for all samples independent of graft materials, impaction levels and load blocks, subsidence occurred logarithmically and that elastic recoil was minimal. Therefore the subsidence versus cycles curves between start and end point of each load block did not reveal additional information but confused the readability of a chart as represented in figure 7.14 (left). Thus in the following figures cone subsidence is only documented by linearly connected data points giving the cone positions at the start and end of each load block as shown in figure 7.14 (right). It can be seen that such a simplified data representation improved readability without losing information.

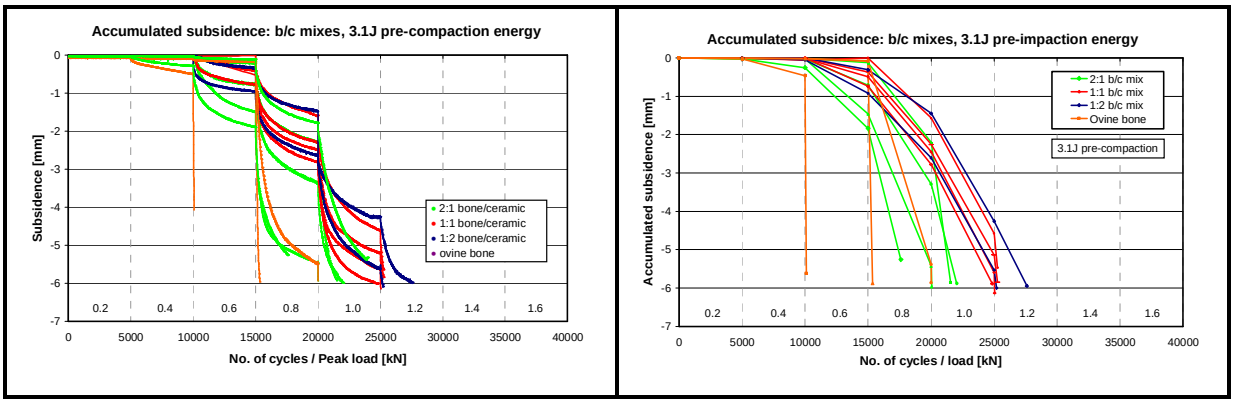

Figure 7.14: *Comparison of two equivalent chart styles showing the accumulated stem subsidence as continuous curves (left or a connection of load block end positions (right).*

The first stability comparison was performed between human bone graft as the gold standard in clinical impaction grafting and ovine bone graft as the preferred *in-vitro* experimental graft used in this study. Figure 7.15 shows that all three human bone graft samples were highly stable without significant subsidence during the first two load blocks but then subsided massively during the 0.6kN load block to finally fail after a few further cycles under 0.8kN peak force. Also ovine bone graft samples were initially very stable without much subsidence but then sudden massive subsidence occurred leading to failure within two further load blocks. Despite this qualitatively similar subsidence behaviour, all but one of the six ovine bone samples tested were more stable than the human bone samples. Cones impacted into ovine bone graft exceeded the failure criterion during the 0.8kN, 1.0kN or 1.2kN load block surviving between 15,425 and 25,405 cycles. This relatively large range indicates the high variability in the stability performance of ovine bone graft especially when the relatively large discrete jumps in peak force from between load blocks are considered. Human bone samples only survived between 15,100 and 15,470 cycles. Variability seems lower but the step size in peak force between load blocks is relatively larger.

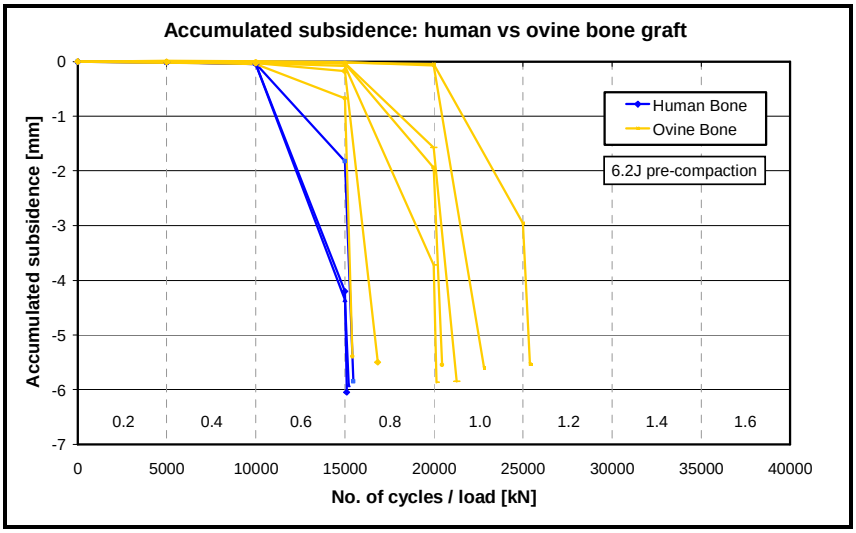

Figure 7.15: *Comparison of accumulated stem subsidence during block loading for pure human and ovine bone graft both pre-compacted with the standard 6.2J pre-compaction energy.*

At the highest pre-compaction level delivering 23.3J of hammer energy into the graft prior to cone impaction, human bone graft showed high absolute stability as represented in figure 7.16. The most stable human graft sample survived for 30,231 cycles before exceeding 6mm subsidence during the 1.4kN load block. With nearly twice the number of cycles to failure and nearly double the peak load, increasing graft compaction energy caused a very substantial stability improvement for human bone grafts. Such improved graft compaction also significantly increased the stability of ovine bone graft so that it remained more stable than its human source derivative. With 45,590 to 60,059 cycles to failure at either 2.0kN or even 2.6kN peak force, stability values nearly doubled but variability remained. The ovine graft sample exceeding 60,000 cycles to failure was the most stable sample tested and indicates that dense impaction leads to high stability with bone grafts. The characteristic of bone grafts to maintain stability without significant subsidence until a certain peak force and to then suddenly subside massively was maintained at the high impaction level.

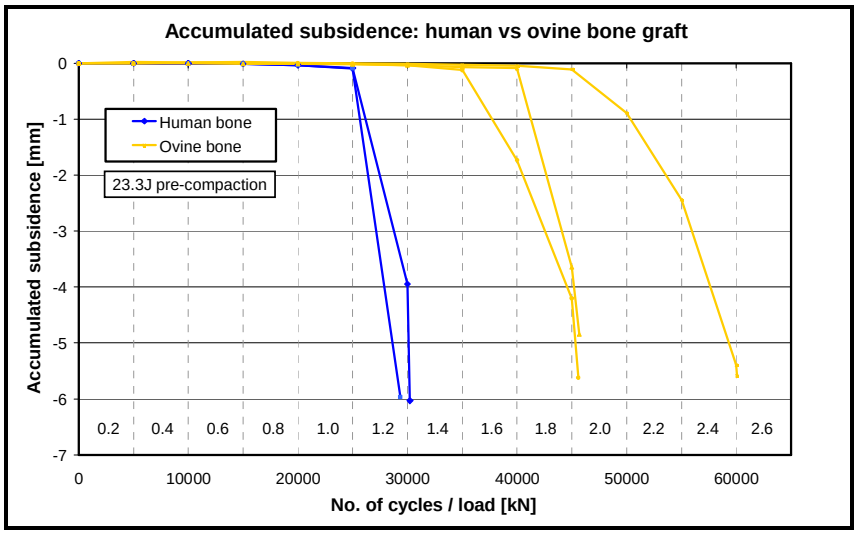

Figure 7.16: *Comparison of accumulated stem subsidence during block loading for pure human and ovine bone graft both pre-compacted with the highest pre-compaction energy of 23.3J.*

The stability performance of a graft mix containing equal volumes of morsellised ovine bone and a granular ceramic extender of the standard configuration, a 80:20 HA/TCP composite sintered at 1150°C with 25% porosity and a 2-4mm particle size, is represented in figure 7.17. Adding the synthetic extender into a 1:1 b/c mix hugely increased stability over pure bone grafts. Even the weakest sample survived 35,294 cycles up to a 1.6kN peak force, a minimum increase of nearly 10,000 cycles and two load blocks (0.4kN) between the most stable ovine graft sample and the least stable b/c graft mix. The variability in stability was also much reduced for the graft mixes. The most stable 1:1 b/c mix only survived 5,298 cycles and one load block more than the weakest sample, a relatively minor difference when the relatively small step size at such high peak load is considered. Most samples recorded even closer stability performances. Subsidence for the b/c graft mixes also was much less sudden or steep and thus more predictable than for the pure bone grafts. After the initial subsidence had

exceeded ca. 0.2mm during the 0.8kN load block, the bone/ceramic mix samples subsided at relatively low and slowly increasing rates towards late failure while the pure bone grafts in this situation collapsed almost totally within one load block.

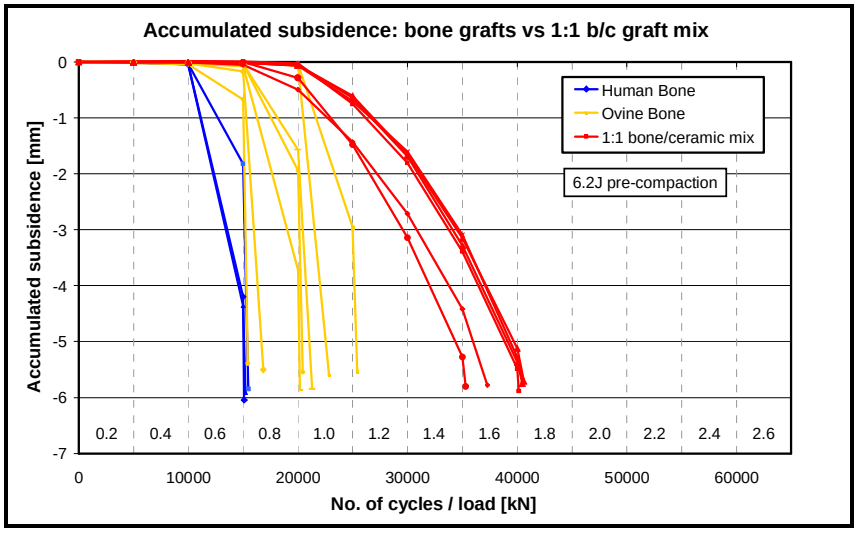

Figure 7.17:
Comparison of accumulated stem subsidence during block loading for pure human and ovine bone graft versus a 1:1 bone/ceramic graft mix (6.2J pre-compaction energy).

The characteristic differences between the qualitative and quantitative stability performance of different grafts can be understood when the subsidence curves of a 1:1 b/c mix are compared to those of pure bone and the standard ceramic as their two constituents (figure 7.18). When a cone is impacted into pure granular ceramic, the 6mm failure subsidence was reached even later then for the 1:1 mix. Subsidence rates were even less steep, increased more slowly and relative variability was lower. Failure for the least and most stable pure ceramic sample occurred in a small range of 45,794 (2.0kN) and 51,382 (2.2kN) cycles only. However, the ceramic subsidence curves intersect those of the 1:1 b/c graft mix and those of pure ovine bone because initial subsidence of ceramic samples during low force load blocks was higher.

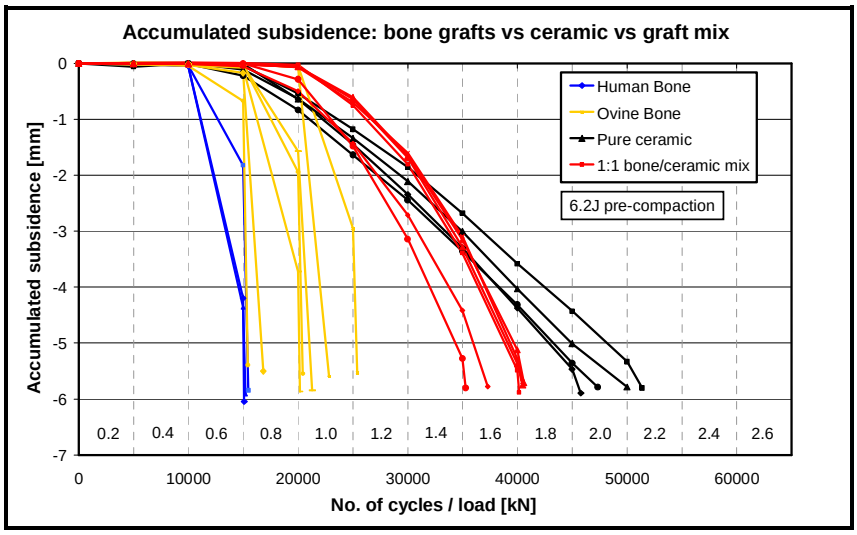

Figure 7.18:
Comparison of accumulated stem subsidence during block loading for pure bone grafts, the pure standard ceramic and a 1:1 bone/ceramic graft mix.

Figure 7.19 proves that not all ceramic graft configurations increase the mechanical stability of a bone/ceramic mix versus a pure bone graft. When a pure HA ceramic with 68% porosity and a 2-5mm particle size produced by an alternative manufacturer was added to ovine bone graft in a 1:1 volume ratio, the average stability of the composite was lower than for pure bone graft. Five from the seven ovine bone samples survived a higher number of cycles and a load block with a higher peak force than the most stable 1:1 b/c mix with pure HA. Graft mixes with the pure HA granules also exhibited the typically sudden and massive subsidence observed for pure bone.

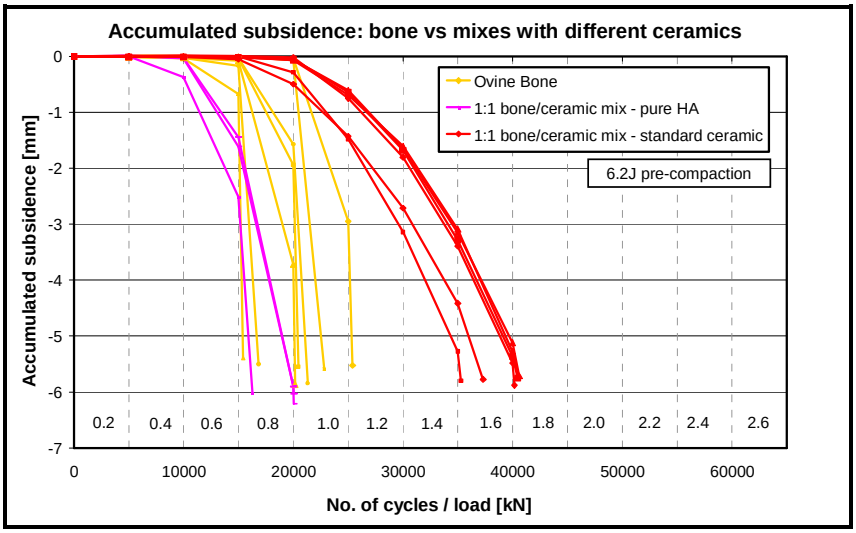

Figure 7.19:
Comparison of accumulated stem subsidence during block loading for pure ovine bone and two 1:1 b/c mixes, one containing the standard ceramic and one containing a highly porous HA.

When the pre-compaction energy was raised from the standard 6.2J to the highest level of 23.3J and with it the total impaction energy, the mechanical stability of pure bone grafts and bone/ceramic mixes is shown in figure 7.20. In comparison to figure 7.17 (6.2J pre-compaction) the subsidence curves of human bone, ovine bone and the 1:1 b/c mix were all shifted significantly towards higher stability. In particular the stability of the both bone grafts was strongly increased with human graft samples exceeding a minimum of 29,360 cycles at 1.2kN against a previous maximum of 15,470 cycles at 0.8kN. Ovine bone exceeded a minimum of 45,590 cycles at 2.0kN against a previous maximum of 25,405 at 1.2kN. The average stability of the 1:1 b/c mix also improved significantly when impaction energy was raised to the maximum but the effect was less strong. The weakest sample of the high impaction energy group withstood block loading to 45,240 cycles at 2.0kN peak force and thus was only slightly more stable than the strongest sample of the standard impaction energy group (40,592 cycles, 1.8kN). As a result of the different stability increases with intensified impaction, the stability difference between pure ovine bone and a 1:1 bone/ceramic graft mix was much less pronounced but the b/c mixes remained mechanically superior. The qualitative differences between pure bone and the graft mixes also remained after high energy impaction. Bone grafts remained stable with low levels of accumulated subsidence until relatively high peak loads but

at some point subsided suddenly and steeply towards ultimate failure within a few load blocks and number of cycles. Contrarily, bone/ceramic mixes registered clearly noticeable subsidence of at least 0.6mm subsidence even after the 1.4kN load block when most pure ovine grafts had only subsided by at most 0.12mm. Further subsidence however continued at much lower and more slowly growing rates than those of pure bone. Ultimately, three out of four mix samples failed later than two out of three ovine bone samples.

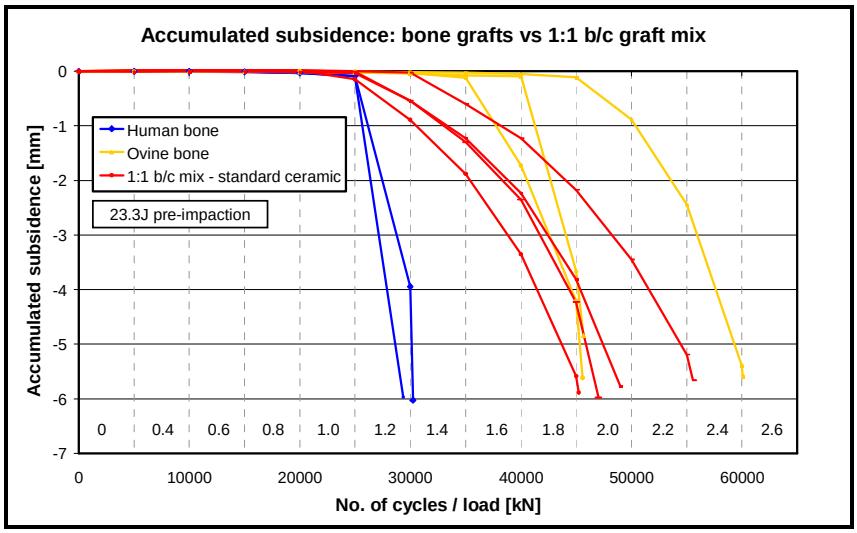

Figure 7.20:
Comparison of accumulated stem subsidence during block loading for pure human and ovine bone graft versus a 1:1 b/c mix (standard ceramic, 23.3J pre-compaction energy).

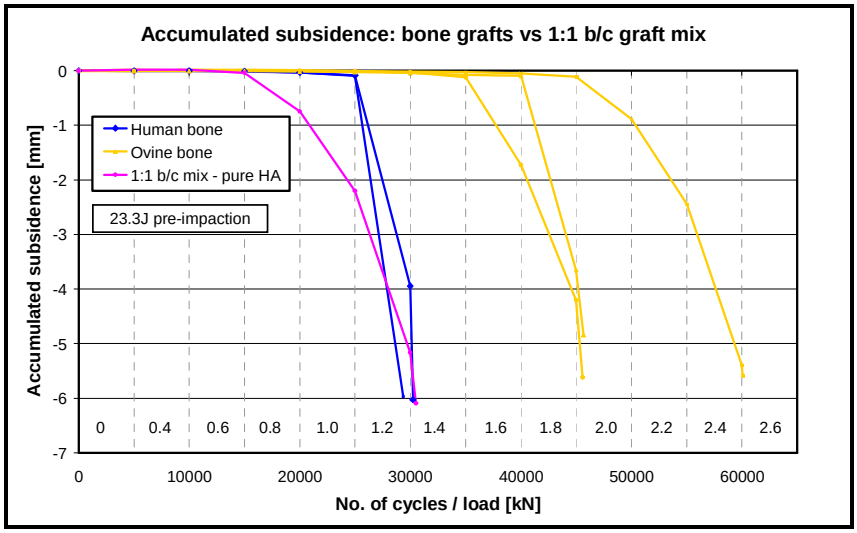

Figure 7.21:
Comparison of accumulated stem subsidence during block loading for pure human and ovine bone graft versus a 1:1 b/c mix (highly porous HA, 23.3J pre-compaction energy).

Figure 7.21 confirms that differences in mechanical stability against vertical cone subsidence measured for grafts at lower levels of impaction energy are maintained at high impaction intensities. The 1:1 bone/extender mix containing the highly porous HA showed inferior stability to pure ovine bone at the standard impaction energy level and despite a stability increase recorded after high energy impaction, the 1:1 b/c mix remained less stable than the pure ovine graft. Cycles to failure were nearly identical to pure human bone, but the ovine bone plus HA mixture exhibited qualitative characteristic typical for the subsidence of all b/c

mixes. Some noticeable early subsidence at low peak loads was followed by subsidence rates lower and more slowly increasing than those of pure bone.

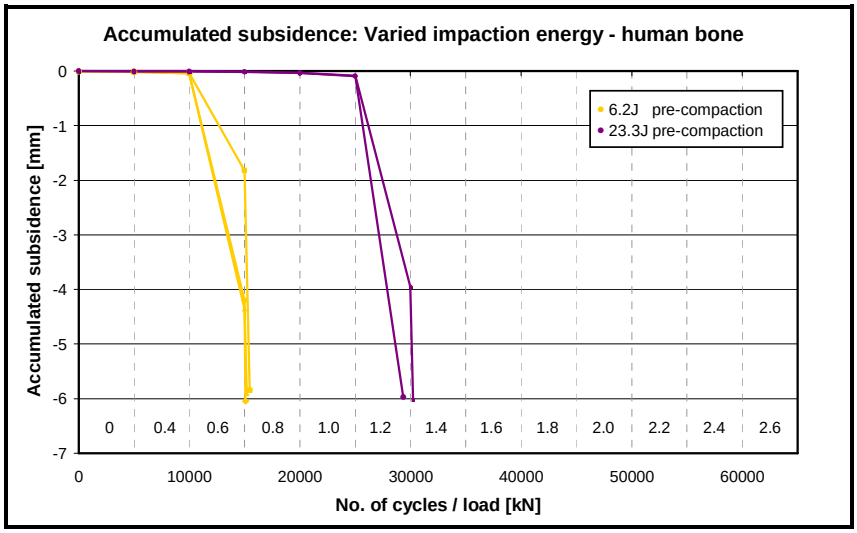

Figure 7.22:
The influence of impaction energy levels on the stability against vertical subsidence for human bone graft pre-compacted with 6.2J (yellow) and 23.3J (violet) energies.

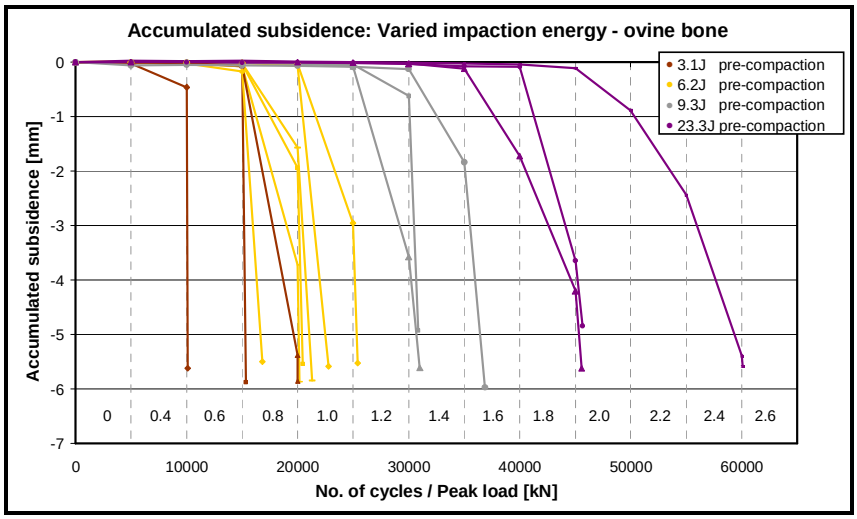

Figure 7.23:
The influence of impaction energy levels on the stability against vertical subsidence for ovine bone graft pre-compacted at 3.1J (brown), 6.2J (yellow), 9.3J (grey) and 23.3J (violet).

Figure 7.22, 7.23 and 7.24 isolate the influence of various levels of pre-compaction energy on human bone (7.22), ovine bone (7.23) and the standard 1:1 bone/ceramic mix (7.24). All graft materials responded sensitively to increased impaction energy with significantly improved stability. Even small step sizes in energy as tested with the ovine bone graft (figure 7.23) raised stability in such a strong way that, despite high stability variability for bone in general, no overlapping subsidence curves were registered except for one sample of the 3.1J energy group. Also the 1:1 bone/ceramic mixes reacted to increased graft compaction with increased stability in such a way that even between the close 3.1J and the 6.2J energy groups no overlapping subsidence curves were recorded (figure 7.24). The characteristic qualitative subsidence behaviour of pure bone and graft mixes was maintained for all impaction levels. The course of subsidence from shallow to steep for pure bone and the slow continuous rate increase for bone/ceramic mixes was maintained as well as the clearly higher variability in

stability for pure bone versus the bone/ceramic mixes. Relative stability differences between graft materials recorded at any one impaction level also remained identical at any other impaction level. The ovine bone grafts were more stable than human bone graft at any tested impaction level but less stable than the 1:1 bone/extender mixes with the standard ceramic at any tested impaction level. Comparing figure 7.23 with 7.24 it can also be seen that adding the ceramic extender to pure ovine bone increased stability most when lower impaction energies are compared. The stabilising effect of the ceramic admixture became less when the extreme pre-compaction energy of 23.3J was applied.

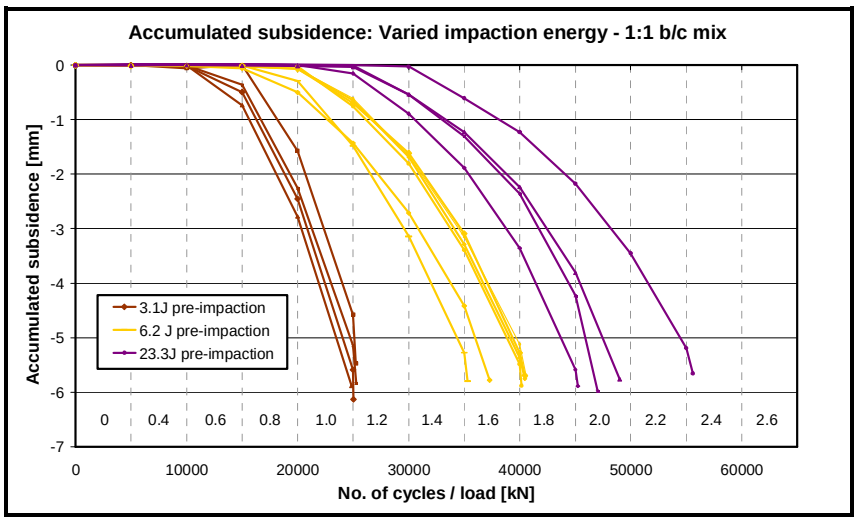

Figure 7.24:
The influence of impaction energy levels on the stability against vertical subsidence for a 1:1 bone/ceramic mix with the standard ceramic pre-compacted at 3.1J (brown), 6.2J (yellow) and 23.3J (violet).

Impaction energy was identified as a crucial influence on graft stability. The effect of different impaction forces delivered by different hammer momentums was analysed in figure 7.25. Graft samples of the standard 1:1 b/c mix were prepared with identical pre-compaction energy levels of 6.2J but those were delivered by hammer blows from different drop heights and thus different hammer momenta of 0.7, 1.0, 1.4 and 2.0Ns. As figure 7.25 shows, a low hammer momentum of either 0.7Ns or 1.0Ns resulted in lower graft stability than when high impaction forces were employed by a hammer momentum of either 1.4Ns or 2.0Ns. However the differences were secondary when compared to the effects impaction energy had on stability. A very high impaction force equivalent to a hammer momentum of 2.0Ns did not deliver higher graft stability than the 1.4Ns hammer momentum but was even slightly less stable. Obviously the relationship between hammer force and stability was not linear and relatively weak. A medium impaction force was identified to deliver maximum stability.

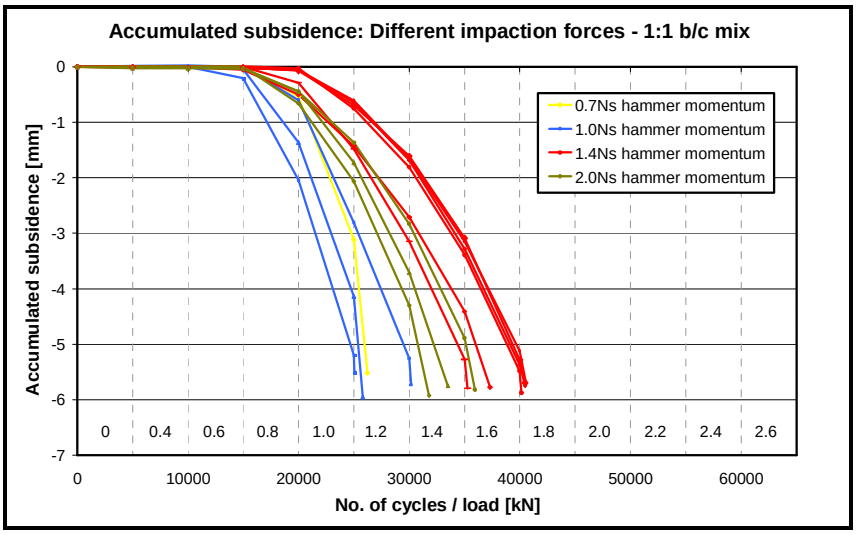

Figure 7.25:
The influence of hammer force or momentum during constant energy impaction on the stability against vertical subsidence for a 1:1 bone/ceramic mix.

The question of how different mixing ratios between bone and the standard ceramic graft extender influence the stability of bone/ceramic mixes was investigated for low pre-compaction levels (3.1J, figure 7.26) and the standard pre-compaction energy (6.2J, figure 7.27 and 7.28). For both impaction levels, adding the standard ceramic granules to bone graft to produce 2:1 bone/extender mix resulted in significantly increased stability against subsidence. At the low impaction level three out of four 2:1 b/c mix samples survived longer than the most stable sample of the highly variable pure bone graft group. At the standard impaction level all three 2:1 mix samples were at least as stable as the longest surviving pure bone graft sample which marked the stability peak of a large range of results recorded for bone.

Adding the synthetic extender into a graft mix of a relatively low ceramic content reduced variability significantly at both impaction levels. At low impaction energies the range of cycles to failure varied from 10,085 at 0.6kN to 20,013 at 1.0kN for pure bone, while the stability of 2:1 b/c mix samples only ranged between 17,600 cycles at 0.8kN to 23,880 at 1.0kN. At the standard impaction level stability values of pure bone varied between 15,425 cycles (0.8kN) and 25,405 (1.2kN) while the 1:2 b/c mix samples showed more consistent mechanical performance with cycles to failure ranging from 25,240 (1.2kN) to 31,296 (1.4kN). In both cases, the bone/ceramic mixes were less variable in absolute and in relative terms especially when the non-linear scale of a block loading experiment with its discrete steps in peak load is considered. Adding only a small amount of ceramic granules into the bone graft was found to increase stability and reduce variability.

The trend towards higher stability and even less variability continued when the ceramic content was raised to a 1:1 b/c mix as shown for both impaction levels. However, raising the extender ratio further to a 1:2 b/c ratio did not show further significant improvement of both stability and variability as seen in figure 7.26. Nevertheless, such a 1:2 b/c graft mix was the

longest surviving sample and even the weakest sample of the high ceramic mix lay well in-between the 1:1 b/c mixes. Thus increasing the ceramic content of a graft mix did at least maintain the stability level of the mixtures with a lower ceramic fraction.

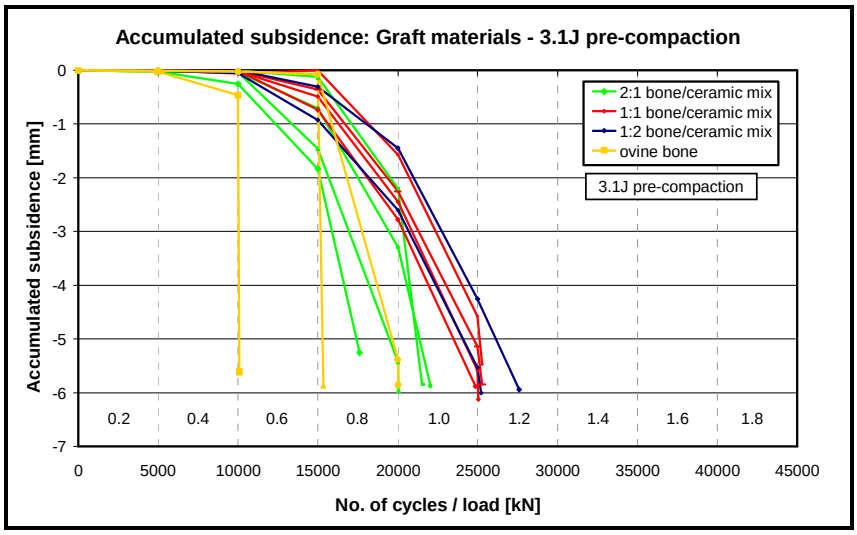

Figure 7.26:
The influence of graft mixing ratios on the stability against vertical subsidence for a 2:1, 1:1 and 1:2 b/c mix of ovine bone and the standard ceramic (3.1J pre-compaction energy).

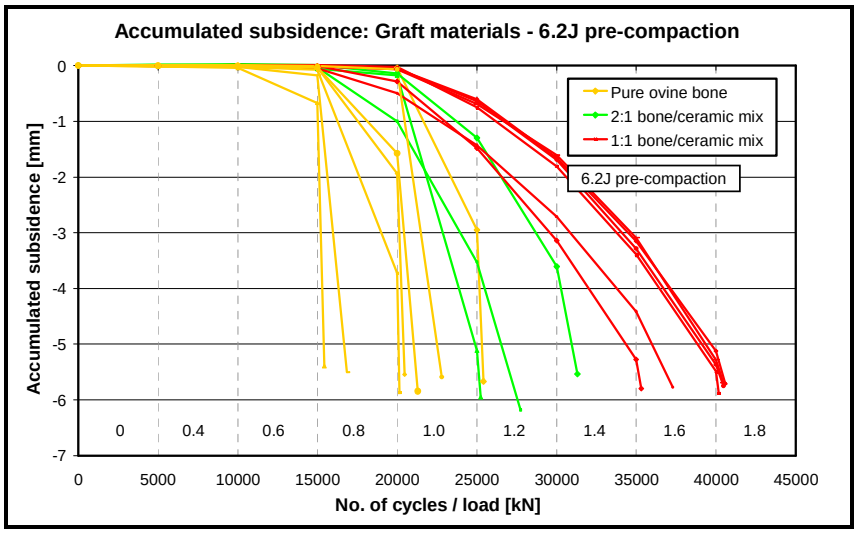

Figure 7.27:
The influence of graft mixing ratios on the stability against vertical subsidence for a 2:1, and a 1:1 mix of ovine bone and the standard ceramic (6.2J pre-compaction energy).

Figure 7.28 shows how qualitative and quantitative properties of the constituents in a bone/ceramic mix combined depending on the mixing ratios. Subsidence curves of pure ovine bone and pure granular ceramic plus the 2:1 and 1:1 bone/ceramic mixes composed of these components are superimposed and it can be seen how the high stability of ceramic granules and the relative low stability of pure bone combined to form mixes with intermediate stability levels correlating with the mixing ratio. The same blending effect of properties was observed for variability and the characteristic subsidence patterns of bone and ceramic. The initially slow subsidence followed by a sudden and steep drop for pure bone grafts and the slowly increasing subsidence rates of pure ceramics blended into each other to form subsidence curves with those qualitative features combined as a function of mixing ratio.

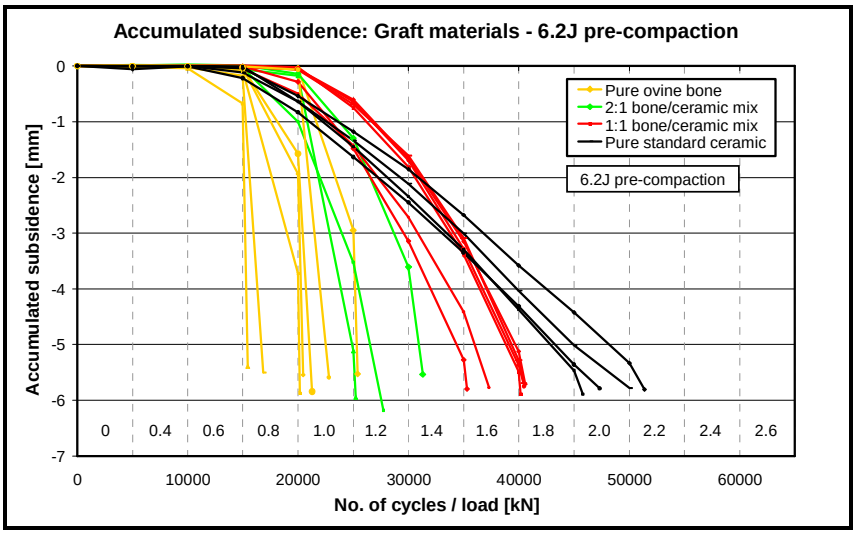

Figure 7.28:
Comparison of stability against vertical subsidence for 2:1 and 1:1 b/c graft mixes and their pure constituents ovine bone and the standard ceramic.

When ovine bone graft was mixed with a highly porous HA graft extender from an alternative manufacturer, the relationship between ceramic fraction and stability reversed in comparison to the standard HA/TCP ceramic (figure 7.29). Compression tests (chapter 4) identified the HA granules as less stiff than bone and the higher their volume ratio in the graft mix the earlier maximum subsidence was reached. While all 1:2 b/c mixes failed during the initial cycles of the 0.8kN load block, all samples with a reversed mixing ratio of 2:1 b/c survived loading up to the 1.0kN load block. The graft mix containing equal volumes of ovine bone and the highly porous pure HA produced subsidence curves which lay exactly in-between.

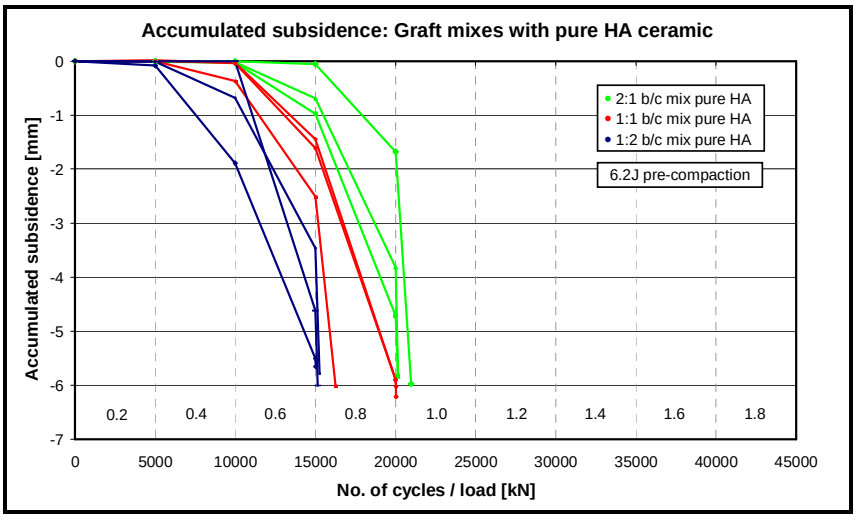

Figure 7.29:
The influence of graft mixing ratios on the stability against vertical subsidence for a 2:1, 1:1 and 1:2 b/c mix of ovine bone and highly porous HA.

The following four charts in figures 7.30 to 7.33 analyse the effects different ceramic configurations such as porosity, sintering temperature, particle size or chemical composition had on the stability of 1:1 bone/ceramic mixes. Porosity had a strong effect on the stability performance of graft mixes when it was raised to biologically desired high levels as shown in figure 7.30. Graft mixes prepared with ceramic granules containing 50% porosity were much less stable than the samples with both low (25%) or no porosity. The two least stable mixes

with the high porosity ceramic survived only 25,181 or 25,490 cycles during the 1.2kN load block and thus only delivered stability levels similar to the most stable pure bone sample which failed after 25,405 cycles at 1.2kN. At the same time, the longest surviving sample of the highly porous ceramic failed one load sequence earlier than weakest sample of the graft mixes with less or non-porous ceramics. Nevertheless, the average stability of the bone plus highly porous ceramic mix was still significantly superior to pure bone graft.

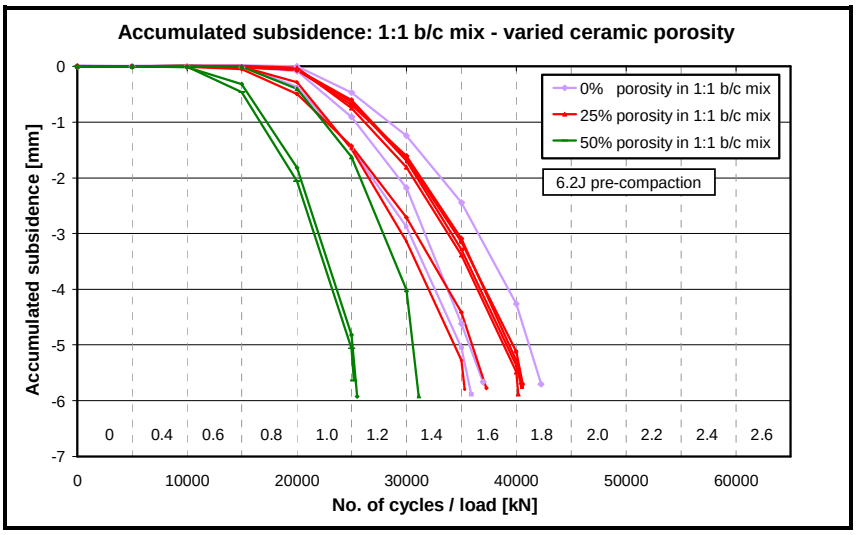

Figure 7.30:
The influence of ceramic porosity on the stability against vertical subsidence for a 1:1 bone/ceramic mix.

No significant stability difference could be identified when the non-porous or the medium porous (25%) ceramics were blended into a 1:1 b/c mix. As expected, a sample mixed with the non-porous ceramic was the most stable but at the same time the other two samples of the group were just slightly more stable than the weakest graft samples containing 25% porosity ceramic granules. As a consequence the stability of graft mixes with the hard non-porous ceramic showed higher variability than the mixes containing the less porous granules.

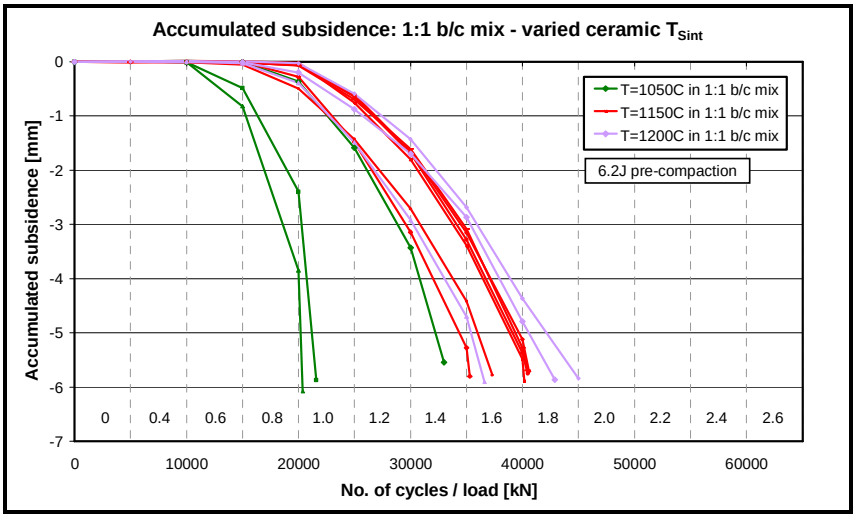

Figure 7.31:
The influence of ceramic sintering temperature on the stability against vertical subsidence for a 1:1 b/c mix.

The effect of ceramic sintering temperature on the stability of 1:1 b/c graft mixes was similar to the observations made for varied porosity as can be seen when figure 7.31 and 7.30 are compared. A very low sintering temperature of only 1050°C resulted in a highly variable and on average low graft stability, lower even than for the highly porous ceramics. The two least stable samples of the low-T_{Sint} mix group only survived into the 0.8kN load block and failed after 20,395 and 21,586 cycles respectively. As a result they were less stable than the longest surviving pure bone graft sample (25,405 cycles; 1.0kN). However, the average stability of even this particularly weak and highly variable graft mix was higher than for pure bone graft. Increasing the sintering temperature to 1150°C massively increased stability and reduced variability so that such graft mixes survived between 35,294 (1.6kN) and 40,592 (1.8kN) cycles compared to the 20,395 (1.0kN) to 33,006 (1.4kN) cycles for the mixes containing low-T_{Sint} ceramics. Raising the sintering temperature further to 1200°C increased stability further so that two out of three samples were more stable than the longest surviving sample from the standard mix group. The stability increase however was relatively small and the variability of high-T_{Sint} ceramic mixes was comparatively high. A similar observation was described when ceramic porosity in the graft mix was reduced from 25% to 0%.

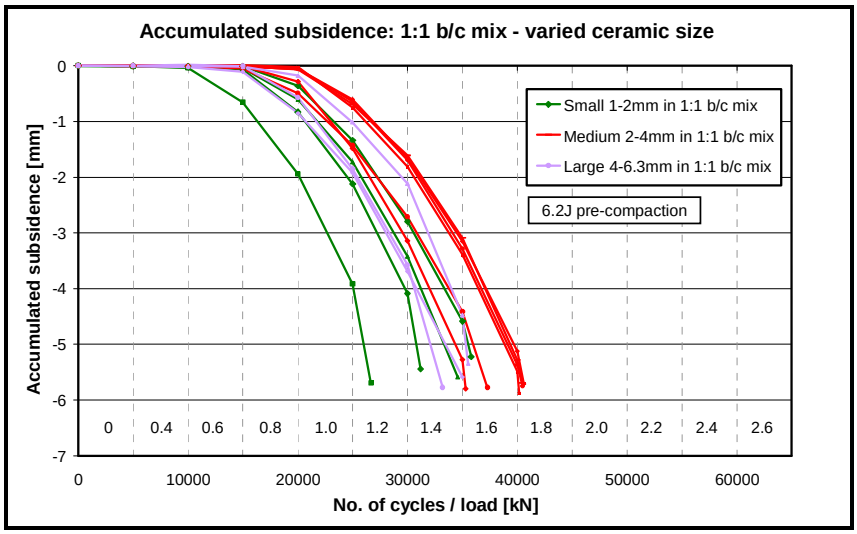

Figure 7.32:
The influence of ceramic granule size on the stability against vertical subsidence for a 1:1 bone/ceramic mix.

When the particle size of the ceramic granules was varied in a 1:1 bone/ceramic mix the effects on stability were less intense than when porosity or sintering temperature were altered. As can be seen in figure 7.32, the stability ranges produced by the mixes containing small 1-2mm particles, medium 2-4mm particles and the large 4-6.3mm granules were overlapping so that differentiation of graft stability levels was less obvious. Nevertheless a certain trend could be identified when the discrete gains in peak force between load blocks were considered. Two of the four samples mixed with fine ceramic particles were clearly the least stable grafts failing after 26,665 cycles during the 1.2kN load block and after 31,194 cycles at 1.4kN. At the same time four of the six graft mixes prepared with the medium sized particles

failed later during the 1.8kN load block and thus were clearly the most stable samples of the tested lot. Although increasing the ceramic particle size from fine to medium improved graft stability, raising it further did not lead to even higher stability but it decreased again. Two of the three samples containing large ceramic granules failed during the 1.4kN load block at a lower peak force and a lower number of cycles than the least stable sample from the medium size group. Even the most stable mix containing large ceramic granules was just as stable as the weakest graft mix containing medium sized granules (35,531 against 35,294 cycles). In comparison to the graft mixes prepared with fine granules, the large granule mixes remained slightly more resistant to subsidence. Thus the stability ranking with reference to particle size was close and identified medium sized granules as mechanically superior to coarse particles which offered slightly more stability than fine granules.

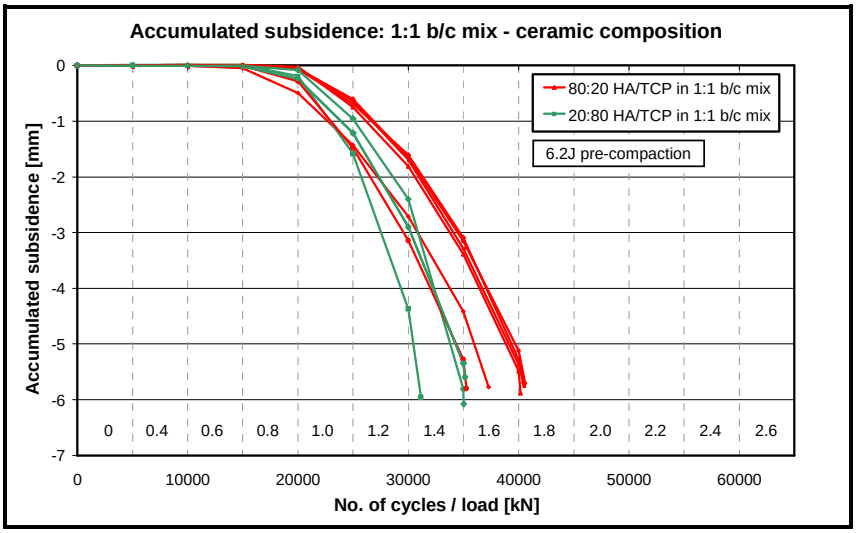

Figure 7.33:
The influence of ceramic chemical composition on the stability against vertical subsidence for a 1:1 b/c mix.

The effect chemical composition of the ceramic phase in a 1:1 bone/ceramic mix had on stability is shown in figure 7.33. Reversing the chemical composition from a HA dominated 80:20 HA/TCP composition to a TCP dominated 20:80 HA/TCP ceramic reduced stability slightly but significantly. However, the effect was much less pronounced than when porosity or sintering temperature were varied. The most stable graft mix containing granules rich in TCP failed after 35,164 cycles at 1.6kN and was just as stable as the weakest sample of the HA dominated ceramic mixes (35,294 cycles). A summary of the main results is given in table 7.1

- Different graft materials and impaction process parameters resulted in a large bandwidth of stability levels measured.
- Cone subsidence showed qualitative characteristics identical for all graft materials and impaction process parameters tested:
  - o Within each load block subsidence increased exponentially with the number of cycles.
  - o Subsidence settled into a constant logarithmic rate causing permanent subsidence.
  - o The subsidence rate was a function of peak load, graft material and impaction parameters.
  - o Subsidence rates and thus subsidence per load block increased steadily between load blocks when the peak force was raised.
  - o During low force load blocks permanent subsidence was minimal or non-existent.
- Qualitative subsidence was very similar for the human and ovine scaled models.
  Significant differences were:
- o *Within load blocks:* The constant logarithmic subsidence rate was reached after less cycles during tests with the ovine than with the human model.
- o *Between load blocks:* With the ovine model significant subsidence occurred already at low peak loads but increased slowly towards higher peak forces. With the human model subsidence at low forces was smaller or non-existent but rates increased more rapidly towards higher forces.
- o Elastic recoil was higher with the ovine than with the human model.
- Stability (cycles to failure) was nearly identical for the ovine and human model.
- Ovine bone graft was more stable than human bone at low and high impaction levels.
- Stability of bone grafts was highly variable.
- Graft mixes with the standard HA/TCP ceramic increased stability and reduced variability.
- In comparison to bone, pure HA/TCP ceramic grafts showed higher subsidence at low forces but rates increased slower towards higher peak loads. Total stability was higher.
- Not all ceramics increased the stability of graft mixes: Adding the highly porous HA ceramic graft decreased stability. The higher its volume fraction the lower its stability.
- Impaction energy is the most influential single factor for graft stability.
- At very high impaction energy levels, pure bone grafts became very stable.
- The stabilising effect of adding HA/TCP ceramic graft extenders was particularly strong at low impaction energy levels.
- Raising the hammer momentum (impaction force) increased stability to a maximum before it dropped again when a very high force was used.
- The higher the content of HA/TCP granules in a graft mix the higher the stability.
- Already small HA/TCP fractions in a graft mix increased stability significantly.
- The qualitative and quantitative properties of bone and ceramic extender combine in a graft mix according to the mixing ratio.
- Increasing porosity of the ceramic granules decreased the stability of a bone/ceramic mix significantly when a certain porosity level was exceeded.
- Lowering the sintering temperature of the ceramic granules decreased the stability of a bone/ceramic mix significantly when temperature fell below a certain level.
- The sensitivity of graft stability to ceramic granule size was lower than for porosity and sintering temperature. A medium particle size led to the most stable graft mix.
- The sensitivity of graft stability to ceramic chemical composition was the lowest of all material configurations tested. Reversing the HA/TCP ratio affected stability only slightly.

Table 7.1: *Summary of results from endurance testing with the human scales model.*

7.3.2 Torsional stability

Impaction energy, impaction force, bone/ceramic mixing ratio and the configurations of the ceramic phase in a graft mix influenced the stability of an impaction grafted cone against vertical subsidence as described above. The resistance against torsion and rotational displacement co-axial with the cone were determined by measuring the maximum torque required for cone release after test completion. Figure 7.34 displays the peak torque against stability (cycles to failure) as measured for the entire variety of graft materials and impaction variables tested. The stability axis displays the number of cycles to failure and the peak force of the load block. Against this scale all torque data points except those for pure ceramic granules lay on a straight line. This indicated a proportional relationship between vertical and rotational stability independent of impaction level and graft material. When a linear trendline was added using the least-square method, the correlation coefficient of this relationship was calculated at R^2=0.869 (figure 7.35). The correlation coefficient might be even higher if the horizontal axis for vertical stability was not distorted by a discrete, non-linear scale of a load block experiment.

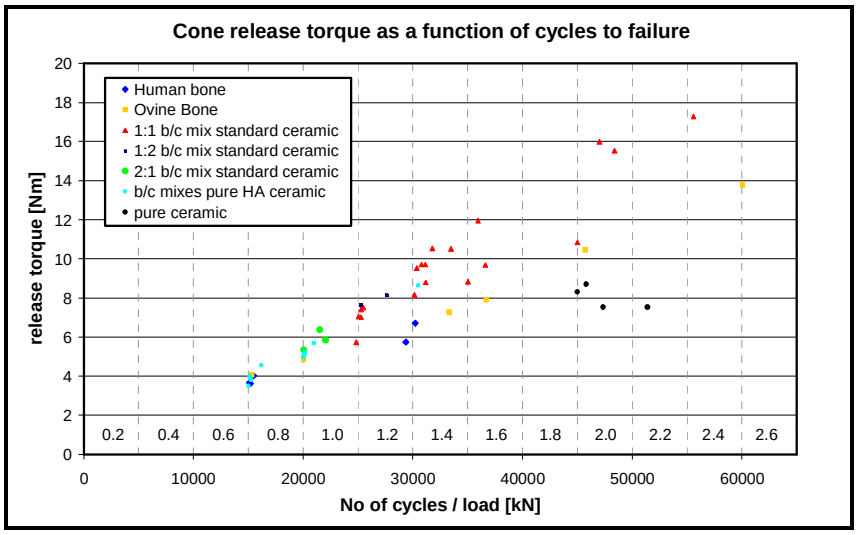

Figure 7.34: *Torque required for stem release after test completion versus stability measured as number of cycles to failure for all graft materials tested.*

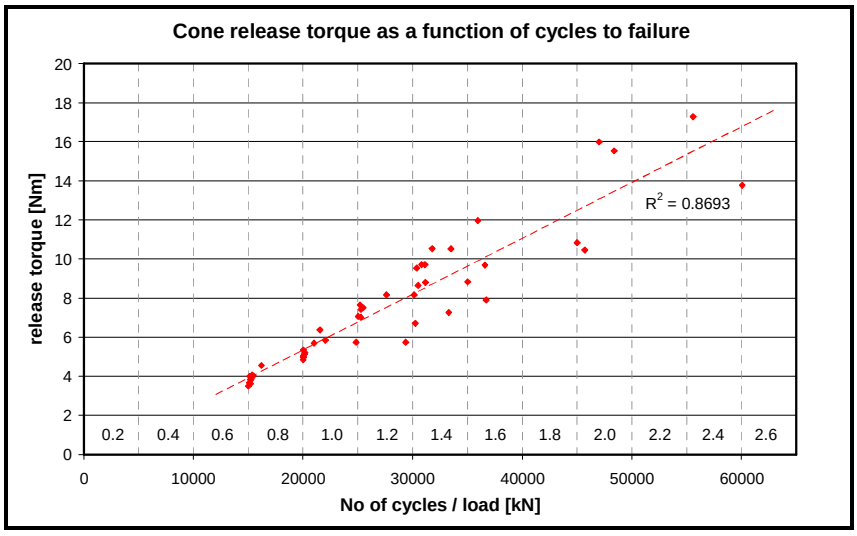

Figure 7.35: *Torque required for stem release after test completion versus stability measured as number of cycles to fai1ure for all graft materials tested excluding the pure ceramic grafts.*

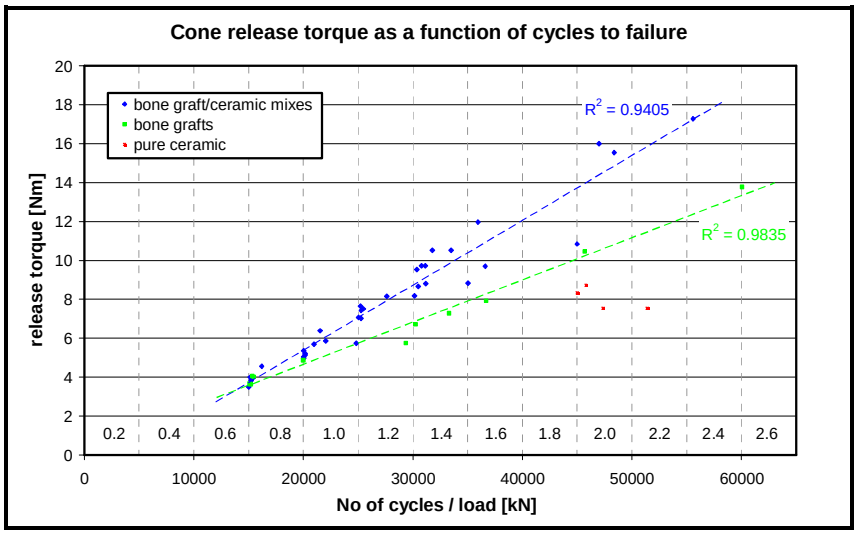

Figure 7.36:
Torque required for stem release after test completion versus stability measured as number of cycles to fai1ure for all graft materials tested.

When in figure 7.36 trendlines were calculated for pure bone grafts (blue) and the bone/ceramic mixes (green) separately, two linear relationships of different slopes were identified. Their correlation coefficients was significantly increased (R^2=0.984 for pure bone grafts and R^2=0.941 for bone/ceramic mixes). The linear function between torsional and vertical stability was slightly steeper for bone/ceramic mixes than for pure bone grafts. The few data points of pure ceramic granules (red) lay outside both functions. This indicates that the functional gradient of torsional versus vertical stability is lower for pure ceramic grafts.

7.3.3 Impaction properties

The impactometer device as described in section 7.1.3 allowed the controlled pre-compaction of graft materials and the controlled impaction of the cone into the pre-compacted graft while permanently monitoring the position of the distal or proximal impactors. This kind of data acquisition allowed the set per hammer blow and the accumulated set to be documented and analysed as a function of graft material or pre-compaction energy level. Figure 7.37 shows how the set of the cone accumulated with the number of hammer blows for three typical samples representing different graft materials and the entire stability range. For all samples tested, like for the human graft and the 1:1 b/c mix samples represented here, the curves of accumulated set versus number of hammer blows followed a logarithmic relationship regardless of pre-compaction energy, graft material or number of hammer blows required for full cone insertion. When the data was displayed against a logarithmic axis for the number of hammer blows, the curves of set versus hammer blows could be approximated as straight lines as shown in the righthand chart of figure 7.37 and in the lefthand chart of figure 7.38. The mathematical relationship followed equation 7.3.

$$x = -\lambda_i * \ln(n) - c \qquad \textit{(equ. 7.3)}$$

x= accumulated set, [x]= mm
n= number of hammer blows
λ_i= impaction rate, [λ_i]= $mm/\ln N$
c= start position constant [x]= mm

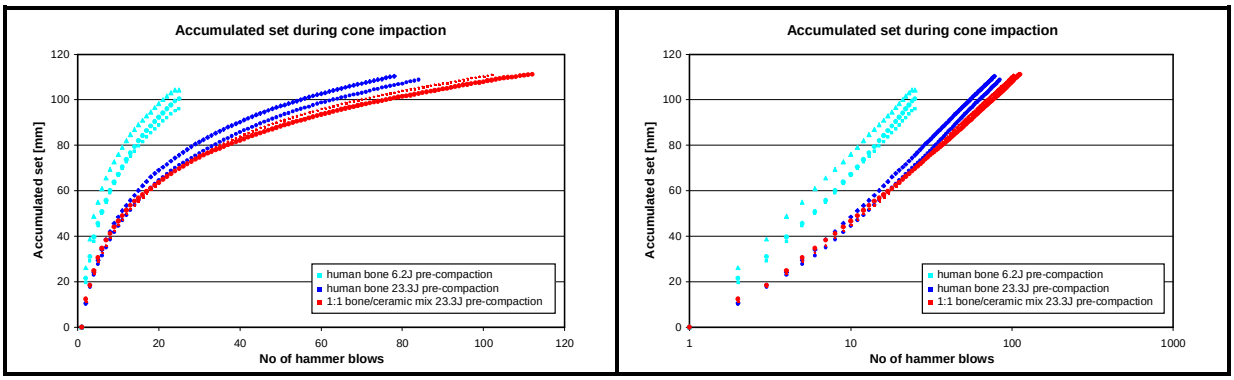

Figure 7.37: *Accumulated set during cone impaction for three samples with very different stability performance under cyclic loading. linear axis (left) and a log.- axis (right).*

Depending on the graft material and on the pre-compaction energy level the logarithmic set versus hammer blows curves were more or less steep altering the impaction rate λ_i. For the three pure human bone graft samples pre-compacted with the standard 6.2J energy and shown in figure 7.37, the cone impaction rate λ varied between 30.59mm/ln(n) and 31.88mm/ln(n) with an average of 31.39 mm/ln(n). For human bone graft pre-compacted with the maximum energy of 23.35J, the average impaction rate was 28.02mm/ln(n) and for the 1:1 b/c mix prepared with the standard ceramic and pre-compacted with 23.3J energy the average impaction rate was only 26.14 mm/ln(n). For samples of such hugely different properties the bandwidth of impaction rates λ_i seemed relatively small. Nevertheless, as figure 7.38 shows with a comparison between impaction rates and stability levels measured during block loading, a clear correlation between impaction rate and stability could be established for those highly different samples. The lower λ_i during cone impaction the longer samples survived during block loading. For less different sample configurations this relationship could not always be identified in the way tabulated and shown for b/c mixes with highly porous HA granules in table 7.2 and figure 7.39 respectively.

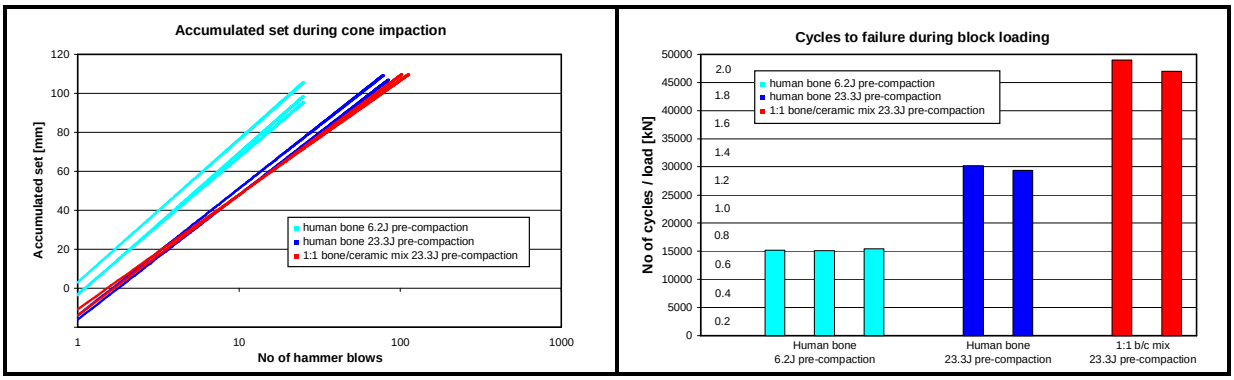

Figure 7.38: *Accumulated set during cone impaction (left) in comparison with stability during block loading (right, cycles to failure) measured for three typical sample configurations.*

Bone/ceramic mix,	**1:2 b/c - *6.2J***	**1:1 b/c - *6.2J***	**2:1 b/c - *6.2J***	**1:1 b/c - *23.3J***
Avg impaction rate λ [mm/ln(n)]	34.58	31.60	31.07	27.95
Avg subsidence 0.6kN [mm]	4.53	1.87	0.57	0.04
Avg No cycles to failure	15,141	18,703	20,430	30,500

Table 7.2: *Correlation between cone impaction rate λ and stability measured as average subsidence after the 0.6kN load block or as the average number of cycles to failure.*

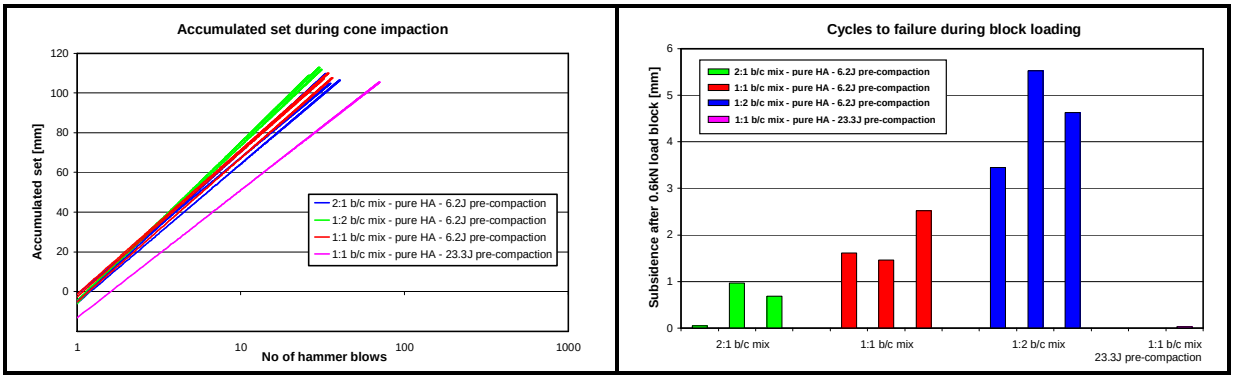

Figure 7.39: *Accumulated set during cone impaction (left) in comparison with stability during block loading (right) measured for different b/c mixing ratios.*

Figure 7.40 displays the set of the final hammer blow (hammer momentum= 1.4Ns) against stability measured as the number of cycles and load block to failure for all pure bone graft samples (left) and all b/c mixes or pure ceramics (right). For both material groups an obvious correlation between set per final hammer blow and mechanical stability became visible.

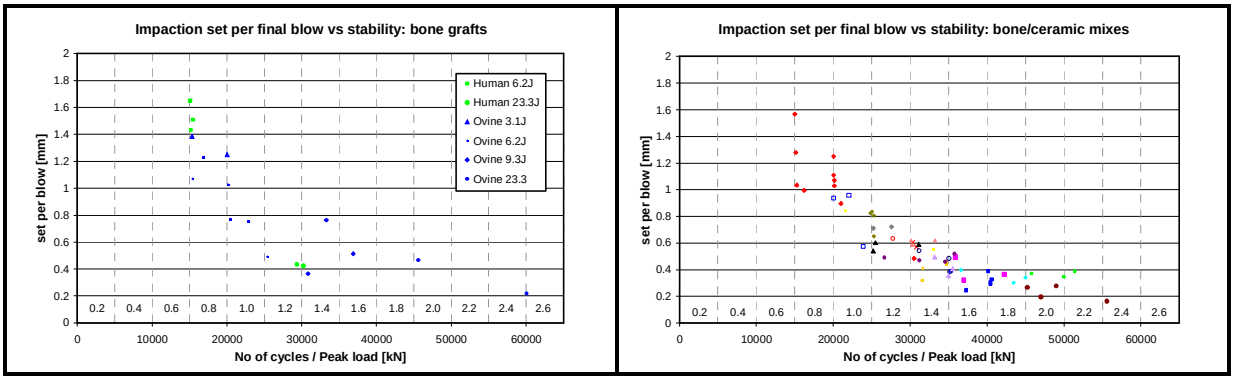

Figure 7.40: *Set per final hammer blow versus stability measured as number of cycles to failure for bone grafts (left) and various ceramic extenders plus b/c mixes (right).*

When the data points of pure bone grafts, pure ceramics, all bone/ceramic mixes and all impaction energy levels were combined into one chart as shown in figure 7.41, it can be seen that the set-stability correlation is entirely independent of graft material and impaction energy level. Despite the non-linear nature of the number-of-cycles axis of a block loading experiment it was possible to approximate the functional relationship between set cycles to failure by an exponential trendline with a high correlation coefficient of R^2=0.997. Set-

stability data points for the samples impacted with different hammer momenta of 1.0Ns (brown) or 2.0Ns (yellow) lay significantly outside the exponential relationship calculated for the medium hammer momentum of 1.4Ns. For identical stability levels, cones impacted with the high hammer momentum scored higher sets per final hammer blow than the samples impacted with the medium hammer momentum and vice versa for the low hammer momentum. It can be expected that the exponential set-stability function only needs to be shifted and skewed appropriately to correlate the set of the final hammer blow and the number of cycles to failure for any particular hammer momentum.

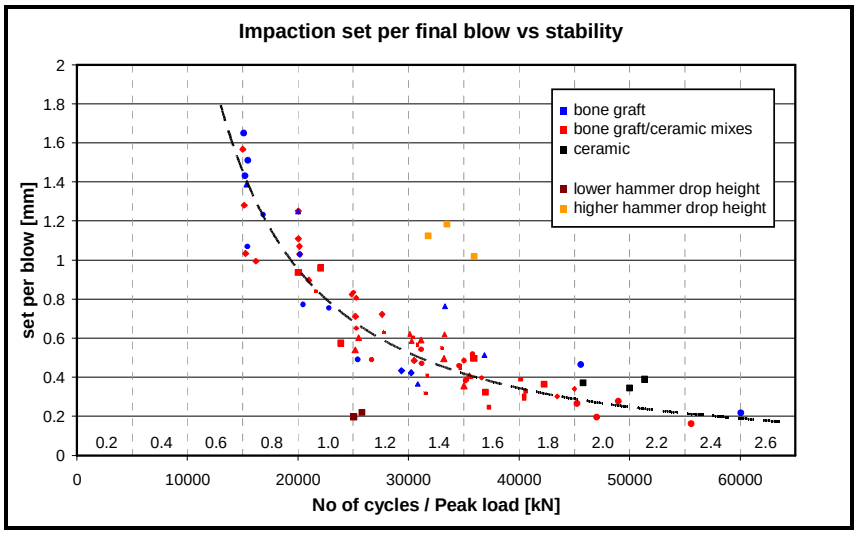

Figure 7.41:
Set per final hammer blow versus stability measured as number of cycles to fai1ure for all samples. An exponential trendline highlights the set-stability relationship.

7.3.4 Sample retrievals

Sample retrieval revealed some qualitative information relevant to the interpretation of load transfer during graft compaction and cyclic loading. After a sample had been cycled beyond the failure point of 6mm accumulated subsidence, it was removed from the test machine and, in the majority of cases, the stem was removed by applying a controlled torque as described above. Then the proximal end plate was removed and attempts were made to remove the graft column within the tube by initially light and later hard tapping of the tube now open at both ends.

With all samples light tapping resulted in a majority of mainly undamaged graft particles falling out the distal end of the tube. A few particles also left the tube at the proximal end. The volume fraction of less densely compacted, mainly undamaged graft removable by such light tapping and the portion of densely compacted graft remaining solidly inside the proximal third of the tube depended on graft material and impaction level applied. Frequent vigorous tapping was required to remove the residual proximal graft mantle. When graft coherence was

broken down this way, the proximal sections did not fall out towards the bottom of the tube but exited against gravity towards the top.

When the cone had not been removed before graft retrieval, light tapping and falling out the tube distally revealed up to 70mm of distal cone section depending on graft material and impaction level applied. When the cone of such a semi-retrieved sample was loaded again in the test machine it seemed that stability against further subsidence had hardly suffered by the removal of such large graft quantities. Stability was mainly provided by the proximal third of the graft mantle. In many cases, further tapping did not remove the residual proximal graft which then had to be scraped away with a tool.

The graft which formed the highly coherent and stable graft mantle in the proximal third of the tube appeared very densely compacted. The majority of particles, in particular the ceramic granules, were fractured into a size range significantly smaller than the original. Highly friable ceramics such as the low sintering temperature HA/TCP or the highly porous HA were entirely destructed to dust-like dimensions. Contrary to expectations, the distribution of bone graft and ceramic extender seemed relatively homogenous throughout the tube. No large concentrations of a single graft phase which might have affected stability could be identified.

7.4 Discussion

Testing graft stability against vertical subsidence under cyclic block loading for a wide range of graft materials and process parameters of the impaction grafting procedure led to a wide range of stability levels measured (Fig. 7.9). Such large differences in quantitative stability performance could only be resolved using a block loading test regime. If a constant peak load had been chosen instead, less stable samples such as pure human bone grafts or less densely pre-compacted samples would have failed immediately after a few cycles. More stable samples such as highly pre-compacted ovine grafts or graft/ceramic mixes might not have recorded any significant subsidence at all. In both cases relative differences in graft stability performance would not have been identifiable. Block loading with a small step size allowed the identification of characteristic subsidence patterns within individual load blocks and their development towards higher forces (chapter 7.4.1). Such information would have been lost if cyclic loading at a constant peak force had been employed.

7.4.1 Qualitative subsidence behaviour

Two qualitative characteristics of subsidence behaviour were identified independent of graft materials and impaction process parameters. Subsidence decreased exponentially with constant logarithmic rates within each load block and subsidence rates increased steadily between load blocks when the peak force was raised. Both the constant subsidence rate within each load block and the slope with which this rate increased towards load blocks of higher peak force could be used as quantitative differentiators between samples of different graft materials and impaction properties. The same observations were made with the ovine model and subsidence with constant logarithmic rates was reported in an implant stability study on human cadaveric femurs as well[227]. This indicates that the subsidence and failure mechanisms at work are the same clinically and for both models despite the altered geometries and dimensions between cone and stem, comparing cemented with uncemented impaction grafting and different loading geometries. The design and process abstractions and simplifications made for the human over the ovine model did not sacrifice any transferability of relative stability comparisons to the more complex *in-vivo* geometry, process and loading regime.

One difference identified between tests conducted using both models was that the constant logarithmic subsidence rates within each load block were reached after fewer cycles with the ovine model (ca. 10) compared to the human model (ca. 10-1000 cycles). Another difference between the models was how the subsidence rates developed towards load blocks of higher peak forces. With the ovine model, noticeable relatively high rates were identified from low peak forces onwards which increased steadily but slowly towards higher peak forces. With the human model however, some stable samples recorded no significant subsidence rates at low force load blocks but rates suddenly increased more rapidly when the peak force was raised beyond a certain level. The point between slow subsidence rates and a sudden increase in subsidence became a characteristic feature during testing with the human model and was more pronounced for pure bone than pure ceramic and b/c mix samples. Additionally, elastic recoil measured with the human model was significantly lower than with the ovine model.

Explanations for these differences must be found in the different geometries and dimensional ratios of stem, cone and tubes and the role of the cement mantle in the ovine model. Stem retrieval after failure of the ovine model samples showed a cement mantle which was strongly attached to the stem. Cement penetration into the compacted bone graft was minimal so that only few graft particles remained attached to the outer cement mantle. Strong stem adhesion, low cement penetration depth indicate that with regard to graft loading, stem and cement mantle do function as one single unit. The cement mantle extends and roundens geometry and

dimensions of the double-tapered stem to form a conically shaped entity with a stiff core and an elastic mantle. The elastic mantle, not present in the human model, should be responsible for the higher elastic recoil measured with the ovine model.

The human model cone and the ovine model stem plus cement mantle differ in taper angles, dimensional ratios between cone and tube diameters, graft mantle thickness, morphology of the distal ends and surface roughness. The extension of the ovine stem by the cement mantle leaves a smaller gap width between the composite cone and the inner tubular surface representing the endosteal wall. With less particles responsible for the load transfer between cone and tube, this geometrical set-up intensifies the loading of the few individual graft particles. Therefore subsidence under vertical loading will initially be steep and rapid as particles become fractured, reorganized and compacted further until a new stability level, e.g. constant subsidence rate is established. With few particles constrained to a relatively small volume and a cement seal suppressing volumetric expansion proximally, graft strains have to be very high for a given stem displacement so that the constant subsidence rates are expected to be relatively low. With the human model, the ratio of tube to cone diameter and thus the graft mantle thickness are comparatively high so that more graft particles are engaged in load transfer. Initial subsidence due to particle fracture, reorganisation and further compaction is slower and it requires more load cycles for an equilibrium subsidence rate to be established. However, once this state is reached in the human model, subsidence rates can be higher than with the ovine model as further graft deformation giving way to stem displacement requires lower graft strains.

Load distribution over a large number of particles also explains why at very low loads the stability of some compacted grafts can be sufficient to almost completely suppress subsidence. This assumption is validated when subsidence rates of pure bone and pure ceramic in the human model are compared (Fig. 7.28). Despite higher ultimate stability of the ceramic, initial subsidence was relatively high at lower peak forces because the brittle nature of the sintered HA/TCP caused particle fractures, reorganisation and further compaction earlier than the more ductile bone grafts. However, the constant subsidence rates established after this process of initial subsidence were lower for the ceramics than for bone as the stability of the reorganised ceramics was then superior to bone.

Size and morphology of the distal ends of the human and ovine model cones could be another reason why the constant subsidence rates in the human model are relatively higher than with the ovine model. The human cone has a sharp and small distal end while the ovine stem/cement-cone forms a smooth and wide tip wedging itself into the graft and cavity left behind by the guide wire with less ease. However this effect should only play a secondary role

because stability is primarily provided by the proximal graft region where the wedge effect of the cone causes intense radial graft compression and stable locking.

As the critical proximal wedge effect is dominated by the taper geometry, the different taper angles formed by both models are also expected to influence stability performance. The human cone has a small taper angel resembling a slim needle-like taper while the ovine stem-cement-cone has a higher taper angle making the cone broader similar to the tip of an arrow. It seems that smaller taper angles such as with the human model maximise radial compression and thus the stabilising wedge effect under cone impaction. The result is high stability with low subsidence rates at lower load blocks. However at higher peak forces, when particles start to fracture, a low angle taper can cause subsidence rates to accelerate faster than tapers with larger angles as seen with the stem/cement-cone of the ovine model. Here cone impaction causes more distal compaction and less radial compaction so that noticeable subsidence occurs already at low loads. At higher loads however, subsidence rates accelerate slower than with low taper angles because vertical subsidence causes a higher degree of vertical compression and thus uses more graft for load transfer than the proximally wedged material alone. Subsidence of a cone with a large taper angle must also deform higher graft volumes per subsidence unit than an acute-angled cone. As both taper angles compared here are still too similar to mark the extremes of a possible spectrum and because two taper angles alone do not allow meaningful interpolation, more tests have to be conducted to understand the crucial matter of taper angles in impaction grafting.

7.4.2 Human and ovine graft

In correlation with the higher stiffness values measured for ovine versus human bone in die-plunger compression tests, fixed ovine bone as the major experimental graft used in this study provided higher stability against subsidence than human bone, the gold standard in impaction grafting. The difference was not only measured at the standard pre-compaction level (Fig. 7.15) but also at the highest pre-compaction energy level (Fig. 7.16) when stability of both bone grafts was significantly shifted towards much higher levels.

Three major reasons can be identified for the different stability. While human bone graft is sourced from mainly elder donors with an often diseased or weak trabecular bone structure, ovine bone graft is produced from young healthy sheep with consistently strong trabecular bone stock. Secondly, diameters of the ovine humeral heads are smaller than the human femoral heads and thus the relative ratio of cortical to trabecular bone is higher for ovine

bone. Cortical bone is stronger than trabecular bone and thus a higher fraction of cortical bone in the morsellised graft could raise stability. Cortical bone is a clinically undesirable component in the morsellised graft as it lacks the porosity required for osteogenetic processes. Thus, during surgery, cortical bone sections are manually picked out. This was done during *in-vitro* experimentation as well, but as many bone fragments consist of trabecular sections attached to cortical bone, in practice some quantity of cortical bone is always present.

Thirdly, human bone graft contains much higher levels of blood and other fluid phases than ovine bone and during the compaction of wet graft significant amounts of impaction energy are used for squeezing out fluids instead of compacting the graft for increased stability. The blood and other fluids act like a viscous damper under the impact-like loading of surgical hammer blows and dissipate energy otherwise used for compaction of a dry graft. The effect was also visible during die-plunger compression testing when wet graft samples were compressed with a non-porous disc or at high strain rates and excessive stiffness values were measured (Fig. 4.7). Ovine bone grafts contain less blood or other fluids than human graft because firstly sheep are drained of blood by the butcher before meat preparation and secondly because the fixation process includes washing and drying of the graft. Such washing and drying does not only reduce the fluid content obstructive to efficient compaction but also removes some of the soft tissue which does not contribute much to the graft's stability. The washing of human graft has been reported in the literature to improve clinical results[224] and this might not so much be the result of the removal of unwanted tissue but more the result of a drier graft allowing more efficient compaction.

7.4.3 Bone graft, ceramic grafts and bone/ceramic mixes

Mixing pure bone graft with the standard HA/TCP extender improved stability and reduced variability (Fig. 7.17). Subsidence of bone/ceramic mixes occurred less suddenly with subsidence rates increasing at much lower rates than with pure bone grafts. Ultimate failure was not so much the result of sudden collapse as with pure bone but it became a steady, more predictable process. However, small subsidence below 0.5mm started earlier for some b/c mix samples than for the pure bone samples. Combined with the slower increase of subsidence rates, the subsidence curves of the mix samples intersected with the steeply dropping bone graft curves. Increased stability, reduced variability, a slow rise in subsidence rates and small but noticeable subsidence identified for bone/ceramic graft mixes were even more pronounced for the pure ceramic samples (Fig 7.18). Mixing pure bone with the ceramic extender

combined properties of both phases (Fig. 7.28) in good correlation to the observations made during die-plunger compression testing (e.g. Fig. 4.46).

During compression testing, the pure HA/TCP ceramics were much stiffer, showed less relaxation but also were much more brittle than bone grafts. As a result ultimate stability of the pure ceramic and the b/c mixes was expected to be higher than for pure bone graft. The ceramic granules contain porosity but to a lower degree than trabecular bone so that ceramic particle fracture gives way to some subsidence but reorganisation and void filling by the fragmented but strong ceramic granules immediately creates a new stable set-up. As a result some early subsidence during the initial cycles caused by brittle fractures is followed by a low subsidence rate which grows slowly towards higher peak loads. The porosity of trabecular bone is higher than that of the ceramic extenders so that collapse of the trabecular bone structures creates larger spaces for significant stem subsidence very suddenly and without allowing stable fragments to reorganise. As a consequence, subsidence is very low at small loads while the compacted non-brittle bone graft is stable but then rapidly accelerates towards sudden failure.

It was postulated that stem migration into b/c mixtures resulted mainly from ceramic fracture and particle reorganisation. Contrary to the visco-elastoplastic, more ductile pure bone graft composite with its high trabecular void volumes, the hardness and brittleness of ceramics do not allow significant plastic deformation. Concluding from this hypothesis, only highly porous ceramics which offer a high void volume for fragmented granules to fracture and fill should behave differently, failing at lower loads and subsiding more suddenly with rapidly increasing subsidence rates similar to bone. This behaviour was in fact observed for a highly porous derivative of the standard HA/TCP ceramic (Fig. 7.30) and more clearly with an extremely porous HA ceramic from an alternative manufacturer (Fig. 7.17 and 7.29). In this case b/c mixes were even weaker than pure bone. At the same time mixes with the highly porous HA ceramic retained the characteristic of noticeable low force subsidence as a result of friability as observed for all ceramic mixes (Fig. 7.21).

The reduced variability in stability for ceramic grafts and b/c mixes relative to pure bone is due to the higher degree of control inherent in the production of ceramic granules in comparison to the sourcing, storing, sterilisation and morsellising of bone grafts. As the bone graft used in most endurance tests came from similarly aged sheep of comparable health, and as graft was prepared by mixing large numbers of humeral heads, variability of bone from two or three human donors as used clinically would be expected to be much greater.

Mixing a ceramic extender into a bone graft adds another phase which complicates homogenous mixing and makes graft preparation and charging prone to a new source of variability. However, despite this risk, the variability of the b/c composite was low and analysis of retrieved samples showed no major concentrations of individual graft phases which would have indicated inhomogeneous mixing.

7.4.4 Influence of impaction energy

Impaction intensity, quantified here by the pre-compaction energy, was the single most important factor influencing the graft stability of all materials. Ovine bone reacted most sensitively to increased impaction intensities (Fig. 7.23) while human bone graft showed less improvements in stability (Fig. 7.22). As discussed above, with human bone the additional impaction energy is less efficiently used for graft compaction and thus stability but hammer blows squeeze out blood and other fluids abundantly present in human bone graft dissipating the impaction energy in a similar manner to the compression of a viscous damper.

Equal volume mixes of bone and HA/TCP also responded with significantly increased stability when the impaction energy was raised. Standing out is the high stability improvement measured for b/c mixes even at the lowest pre-compaction energy level (Fig. 7.24). The ceramic granules add a stiff and non-ductile phase to bone which cannot be significantly compacted and which does not need high compaction to provide high stability. Thus the strengthening effect of adding HA/TCP particles into a bone/ceramic mix is most pronounced at low impaction levels when pure bone responds with far inferior stability.

When the highest impaction energies were employed the stability gain of the ovine bone graft was relatively larger than for the b/c mixes. At the maximum pre-compaction energy, the average stability of the ovine bone was similar to the stability of the 1:1 b/c mixes with the standard HA/TCP. This indicates that pure bone grafts, if well impacted, can provide high stability sufficient for clinical impaction grafting, although variability remains high. The stability increase caused by increases impaction energies for all graft materials indicates that in a loading environment geometrically constrained by a tube and cone *in-vitro* or a stem and a proximally sealed femoral canal *in-vivo*, stability can be achieved for virtually any graft material as long as compaction is intense enough. In theory all materials compression loaded under inhibited transverse strain will after sufficient linear strain eventually become extremely stiff. In impaction grafting the stiffness or stability of the compacted graft must however be sufficient at impaction intensity levels which can be delivered clinically without femoral

fracture and which still result in a packing density of sufficiently high porosity for osteoconductive processes.

Not only impaction energy but also impaction forces influenced stability. When equal amounts of impaction energy were delivered by hammer blows of different momenta and thus peak forces, stability was affected (Fig. 7.25). The momentum-stability correlation was not linear but a medium value was identified to deliver the highest stability. A higher hammer momentum resulted in slightly less stability while the stability lost with lower hammer momenta was significantly higher. It seems that optimum compaction requires an optimum impaction force which will not damage crucial load bearing particles whilst allowing adequate packing through particle deformation and rearrangement. It must be mentioned that peak hammer forces on impact do not correlate linearly with increased hammer momenta because the peak force also depends on the stiffness and damping properties of the system being impacted.

Peak impaction forces can be estimated by the pile driving formula used in civil engineering to estimate the load bearing capacity of a pile driven into soil as given below[206].

$$m \cdot g \cdot h = \eta \cdot F \cdot s \qquad \text{(equ. 7.4)}$$

m: mass hammer	F: supported maximum force
h: drop height hammer	s: set per hammer blow
g: gravity	η: efficiency factor

The equation calculates the impaction force of the dropping hammer by equating hammer energy and work required for the measured pile displacement. In civil engineering the impaction force gives the upper limit of the static force which can be supported after a hammer blow of a certain measured set. Here the equation is used to estimate the peak force delivered by a hammer blow. Using the static stability consideration derived from the pile driving formula, maximum peak forces delivered by the impaction hammer must at least exceed the peak forces during block loading as those forces were not only supported statically but even for a significant number of load cycles. With load blocks peaking at 2600N, the maximum hammer forces are expected to be a multiple of this figure at around 5-10kN. Applying the pile driving formula with values for impaction set ranging between ca. 0.1 and 1mm and assuming an efficiency factor of η=2, maximum peak forces on impact are estimated between 780N and 7.8kN with an average of 3.9kN. Whether such high forces are also achieved during clinical impaction depends on the stiffness and damping properties of the dislocated leg acting as the support against hammer blows during surgery.

7.4.5 Bone/ceramic mixing ratios

Mixing ratios of bone and ceramic graft extender affected stability in correlation with the properties of the individual phases combined. The higher the content of the standard HA/TCP granules in a bone/ceramic mix, the higher stability and the lower variability. Raising the ceramic content from pure bone, via 2:1, 1:1 and 1:2 bone/ceramic mixes to pure ceramic, the largest step in relative stability increase was noticed when pure bone and the low ceramic content 1:2 mix were compared (Fig. 7.26 and 7.27). Stability increased further when the ceramic content was raised but the relative increase tailed off. This observation corresponds well with stiffness measurements during die-plunger compression testing (Fig. 4.46). The stability of compacted graft relies on two major features, good compactability such as provided by the ductile phases in bone graft plus stiff and strong particles for load transfer as provided by the trabecular bone fragments or the ceramic granules. Bone graft in its pure form contains insufficient quantities of strong and stiff particles but too much soft tissue which, as described, requires very high impaction energies to achieve stability. Adding small amounts of hard ceramic granules quickly shifts the ratio between both collaborating phases towards a favourable composition thus increasing stability. Due to the significantly higher stiffness and stability of the HA/TCP phase, raising the ceramic content further increased stability but as compactability is sacrificed at the same time, the relative increase tails off as observed.

The described stabilising effect of a synthetic graft extender only works when the ceramic phase provides particles of strength and stiffness far superior to bone. The highly porous pure HA ceramic graft showed stiffness values in the die-plunger test which were at most equal to bone (Fig. 4.27 and 4.28). Thus adding and raising the content of the highly porous HA in a b/c mix reduced stability (Fig. 7.29). Instead of increasing the fraction of strong and stiff granules, the friability and porosity of the material promoted graft collapse and steep subsidence.

7.4.6 Ceramic properties in bone/ceramic mix

- **Varying porosity of the ceramic phase**

Sensitivity of stability to ceramic porosity was also identified when the pore volume was increased for the standard HA/TCP graft extender (Fig. 7.30). The non-porous ceramic provided the highest stability in a 1:1 bone/ceramic mix. At a medium 25% porosity level, stability was hardly affected but the higher 50% porosity ceramics caused mix samples to fail at distinctively lower peak forces. Porosity increases the friability of granules due to stress raising voids and it enlarges the volume available for graft collapse and subsequent

subsidence so that from a certain porosity level onwards stability is significantly sacrificed. From sample retrievals, handling and from observations made during die-plunger compression testing (Fig. 4.40) it was seen that higher porosity not only increases particle fractures but those fractures also produce much higher volumes of small dust-like fragments. The size of these fragmented particles is in the range of original pore size so that the porosity originally engineered into the material for osteoconductive potential disappears under impaction and loading. Granules of lower porosity levels do not produce as much dust but tend to break up into a few smaller units which still exhibit the original porosity. The low dust production of non-porous particles is more the result of inter-particle friction.

- **Varying sintering temperature of the ceramic phase**

Lowering the sintering temperature had a the same effect on stability as increasing porosity. The highest sintering temperatures caused highest stability. Slightly reduced temperatures almost retained this stability level. However, once sintering temperature dropped below a certain value samples failed early at significantly lower peak loads. At low temperatures sintering is not complete and the cohesion of the original powder weak. This results in high friability very similar to that of a highly porous ceramic. Thus the production of dust-like fragments under impaction and loading is at similarly high levels so that massive subsidence occurs early. Indeed, particle size analysis after die-plunger compression testing showed even higher dust volume fractions for the HA/TCP ceramic sintered at 1050°C than for the variant with 50% porosity.

- **Varying chemical composition of the ceramic phase**

Porosity and sintering temperature are parameters used to optimise the osteoconductive properties of a ceramic graft but both can massively reduce stability. Chemical composition is another ceramic variable with which ceramic resorption and bone remodelling rates can be varied and when the chemical composition of the original 80:20 HA/TCP ceramic was reversed to a 20:80 HA/TCP composition, stability was only slightly reduced (Fig. 7.33). Despite the large difference in compressive strength of pure bulk, non-porous HA and β-TCP (table 3.2 and 3.3), the stability provided by the composite material dropped only slightly when the TCP fraction was raised. When a HA/TCP composite ceramic is sintered from either a 80:20 or 20:80 HA/TCP mixing ratio, multiple phase changes affect the composition and crystallinity of the sintered product. These phase changes could produce a composite material where the compressive strength of the ceramic sintered from powder rich in weak TCP is only slightly lower than the ceramic produced from a powder rich in strong HA. And indeed, the compression moduli measured during die-plunger testing were so close that the 20:80 HA/TCP ceramic was only 10% less stiff than the 80:20HA/TCP standard composition.

- **Varying particle size of the ceramic phase**

With regard to ceramic particle size in a 1:1 bone/ceramic mix, a medium 2-4mm granular diameter was identified to deliver the highest stability (Fig. 7.32). Both large and small particles lead to slightly reduced stability so that the effect of particle size on stability was much lower than impaction intensity, ceramic porosity or sintering temperature. A medium ceramic particle size seems to balance the two mechanisms leading to subsidence, particle fracture and particle migration, in an optimum way for maximum stability. The packing geometry of large particles in a constrained volume such as formed by the stem and femoral canal creates a higher total void volume and larger individual void spaces than smaller particles. Also, contact points between individual particles are less so that load transfer causes much higher contact stresses. As a result, large particles break up and the fragments collapse into the large void spaces; subsidence occurs. Stability of b/c mixes containing large ceramic particles with a size similar to the dimensions of the stem-canal gap might also suffer from unwanted phase concentrations as homogenous charging is impossible under these circumstances. Small particles pack more densely into the narrow gaps between stem and canal so that total void volume and size of the individual voids is comparatively small. However, small particles are more mobile so that they can migrate within the particulate aggregate and rearrange their packing density more easily. Subsidence becomes facilitated. An extreme version of this situation can be described as being analogous to quick sand. Medium sized particles should keep these effects in equilibrium and it might even be possible that balanced fracture and migration under impaction stabilises the graft as packing density is optimised. For the same reason, a mixture of particle sizes appears beneficial.

In comparison to porosity and sintering temperature, the ceramic particle size had small effect on the stability of graft mixes. Intense compaction breaks down many particles to a similar size distributions independent of the original sizes prior to fatigue loading. This effect was observed from sample retrievals and was particularly strong in the main load bearing proximal third of the tube. Here radial compression from the wedging effect of the cone has led to the highest compaction ratios and thus ceramic fractures prior to cyclic loading.

7.4.7 Torsional stability

For all samples a good correlation between stability against vertical subsidence and rotational stability against torsional loading was established. Relating cone release torque to a linear scale of the number of cycles to failure revealed a linear relationship when the pure ceramic samples were excluded (Fig 7.34). The correlation coefficient R^2 was increased when separate

relationships for pure bone grafts and bone/ceramic mixes were calculated (Fig 7.35). The fact that vertical and torsional stability are proportionally correlated indicates that the major mechanisms affecting vertical and torsional stability are fundamentally the same. Stability against axisymmetric torsional loading should be the result of the normal force onto the cone/graft interface and the friction coefficient between the surfaces of the stem and graft mantle. The friction coefficient theoretically only depends on the graft material while the normal force is affected by the impaction intensity and viscoelastic and fracture properties of the graft. If, for instance, graft deformation is dominated by particle fracture or plastic deformation instead of elastic deformation the normal force would be lower as would be the stability against vertical subsidence. This was for instance the case for weakly compacted bone grafts or graft mixtures with highly porous ceramic grafts. The friction coefficient between cone metal and graft material indeed seemed to affect the linear correlation between vertical and torsional stability as different slopes for pure bone, pure ceramic and b/c mixes indicate. For equal stability levels against vertical subsidence, b/c mixes recorded higher stability against torsion than the pure bone samples hinting at higher interface friction when ceramic is added to the bone. Pure ceramics however showed relatively less torsional stability when compared to equally stable samples prepared with pure bone or graft mixes. This observation seems to contradict the finding that ceramic granules in a bone graft mix increase the friction coefficient but pure ceramics lack the elastic component provided by the bone phase so that despite a high friction coefficient the normal force appears to be insufficient to provide high torsional stability. This indicates that graft stability in impaction grafting is the result of complex phase interaction and that optimum stability is provided by a mix.

7.4.8 Impaction properties

After filling and pre-compacting the graft into the tube with a flat disc modelling distal impaction, cone impaction simulating proximal impaction revealed an exponential relationship between number of hammer blows and accumulated set (Fig. 7.37). The slope of this relationship correlated with the stability against vertical subsidence but only for samples with very large stability differences (Fig. 7.38 and 7.39). Lower stability differences could not be resolved as expected because it would otherwise indicate that impaction energy but not graft materials would be the only variable influencing graft stability.

The set per final hammer blow was identified to correlate well with stability against subsidence independent of the graft material or impaction energy used (Fig. 7.41). The relationship was exponential and the curve was shifted for lower or higher hammer

momentum towards lower or higher stability respectively (Fig. 7.42). Pre-compaction energy and graft material must affect stability against subsidence and final hammer set in the same way. A more densely compacted graft or an inherently more stable graft material responds with less final set to the force of a hammer blow in the same way as it does subside less per load cycle under a lower peak force. A similar correlation between hammer set and stability (static) has been established in soil mechanics (pile driving formula).

7.5 Conclusions

From the discussed results important conclusions can be drawn which have relevance either for the *in-vitro* testing or for the clinical application of the impaction grafting technique. Thus two separate sections are used to discuss conclusions from the experimental analysis. First conclusions are drawn which can justify the experimental methodology employed here and which should be considered in the design of future experimental studies. Secondly conclusions are drawn with implications for the clinical application of the impaction grafting technique and with implications for the optimal configuration of a synthetic bone graft extender.

7.5.1 Model/Experimental conclusions

- **Block loading**

Endurance testing of impaction grafting stability for a wide range of bone grafts, synthetic graft extenders and process parameters revealed a large bandwidth of results, an observation in correspondence with the large stability differences reported for clinical results. Only a block loading experiment is able to resolve large differences in stability and qualitative subsidence characteristics under such circumstances. Unless differences can be expected to be small, as for instance when only slightly varied ceramic properties or mixing ratios are compared, a block loading test regime should be chosen to allow complete analysis.

- **Model abstractions**

Impaction grafting stability was tested using an ovine and a human model which differed in design and loading geometry, dimensions, a manual versus a controlled impaction procedure and a cemented versus an uncemented stem fixation. The ovine model simulates more closely the *in-vivo* situation and the human model is abstracted to a higher degree for focussed parameter isolation and improved reproducibility. Nevertheless, comparing results from the both models showed subsidence to be qualitatively identical in principle and quantitatively

similar for both models. Graft loading and failure mechanisms are fundamentally the same for the ovine and human model. It can be concluded that an equally relevant analysis of impaction grafting stability is possible with the simplifications chosen for the human model, an axi-symmetric cone versus a double-tapered stem, renunciation of cementation and axi-symmetric loading versus off-set loading. However, clinical relevance should only be claimed for qualitative and relative comparisons between different graft configurations or impaction variables. A direct transfer of numerical values derived from the human model into the clinical situation is not feasible and was not intended.

Subsidence was the result of collapsing graft giving way to the cone or stem-cement unit of the ovine model. Slight differences in qualitative subsidence between both models identified the different taper angles of the metal cone and the entity formed by stem and cement of the ovine model as the cause, as well as the different dimensional ratios between graft mantle thickness and cone diameter of both models. With cone taper angle and graft mantle thickness relative to stem and granule size recognised as factors influencing impaction grafting stability, different stem shapes and taper angles should be tested for maximising stability. In the case of cemented impaction grafting, the effect of cement mantle thickness must be re-evaluated because of its different function to primary hip arthroplasty. The concept of uncemented impaction grafting seems promising but in this case, a stem design completely different to the size, tapers and surface finishes used for the cemented procedure should be investigated.

- **Vertical and torsional stability**

A good correlation between stability against vertical subsidence and stability against torsional displacement axi-symmetric with the cone was established for different graft materials and impaction intensity levels. With this proven functional relationship and the identification of vertical subsidence as the dominant failure mode even under off-set loading with the ovine model, limiting experimental loading and displacement monitoring to vertical subsidence only seems reasonable. A more sophisticated design allowing torsional loading and displacement measurements does not promise to deliver additional information sufficiently valuable to justify the added complexity and cost. Increasing torsional stability independent of vertical stability should only be possible by altering stem shape and taper angles.

- **Human bone and ovine bone**

Ovine bone graft morsellised with the Norwich mill proved to be more stable than human bone graft because of a lower fluid content improving compaction efficiency, a healthier bone stock of more consistent quality and a higher cortical bone content. Nevertheless, ovine bone graft is highly suited as an experimental graft for *in-vitro* mechanical tests of impaction

grafting stability. Stability differences were relatively small and during compression tests it was seen that human graft provides equal stiffness and thus equal stability potential to ovine bone when it was milled with the Howex mill. Furthermore, compression tests identified bovine bone, another experimental graft alternative considered amongst researchers, to be much stiffer and thus of highly different stability potential to human bone. Stability differences between ovine and human graft could be much smaller still, if human graft as the reference was washed and dried or deliberately included more cortical fragments. Washing and drying is one common clinical procedure while the removal of all cortical bone is not explicitly advised in many surgical protocols. Even with a stability difference remaining, ovine bone is a suitable experimental graft because, if stability improvements can be measured for certain synthetic extenders or impaction techniques using ovine bone, those improvements will be at least equally as strong with the less stable human bone. Relative stability performance measured with ovine graft will remain valid for human graft.

- **Soil mechanics theory**

The ratio between bone or ceramic granule size and the graft mantle thickness constrained *in-vivo* by the femoral canal and cement coated stem and *in-vitro* by tube and stem is very low. Load transfer models in soil mechanics theory are based on the idealised assumption that the extension of the particulate aggregate is infinitely large against the granule size. Therefore experimental designs investigating properties of such particulate matter demand the ratio between maximum particle size and constraint dimensions to exceed a minimum of ten. In clinical impaction grafting and the experimental models employed here graft granule sizes measured up to 10mm so that this ratio could be as low as one and hardly reaches the minimum requirement of ten. Under these circumstances load transfer depends also on the mechanical properties or contact angles of individual particles and not only on bulk properties which can be attributed to a particulate aggregate by using the soil mechanics theories such as cohesion, shear angle or pore pressure. Thus it must be concluded that the mechanical description of stability mechanisms at work in impaction grafting must go beyond soil mechanics theory. In particular Finite-Element-Models which are usually based on such bulk properties must be approached with great care. It must also be accepted that standard experimental techniques of soil mechanics such as the shear box used in this study can reveal only one aspect with limited applicability.

7.5.2 Clinically related conclusions

- **Sensitive technique**

As summarised above, endurance testing of impaction grafting stability revealed a large bandwidth of results when bone grafts, synthetic graft extenders or process parameter were varied only slightly. This result corresponds well with the large stability variations reported from clinical studies and confirms that impaction grafting is a sensitive complex surgical procedure which requires careful optimisation of process parameters and grafts used to be clinically successful. Initial mechanical stability investigated in this study was in particular highly responsive to impaction intensity, bone graft quality and the porosity engineered into a potential ceramic bone graft extender. Clinicians should pay particular attention to these factors.

- **Exponential subsidence**

After an initial settling-in period, during each load block, stem or cone subsidence followed an exponential curve with a logarithmically constant subsidence rate. Only for small peak forces and for highly stable grafts, subsidence during some load blocks was so small that such a logarithmic subsidence rate could not be identified against signal tolerance or noise. However, even in these cases small permanent subsidence was recorded. Consequently, initial mechanical stability is always accompanied by some subsidence which always increases at an exponentially decreasing rate. Thus long term stability only seems possible when graft incorporation and bone remodelling are completed. However, the logarithmically constant subsidence rates cause subsidence to slow down quickly so that, for the number of gait cycles to be expected during the life-time of a patient, a quasi-infinitely stable state can be attained. Therefore some early initial subsidence can be tolerated post-operatively without sacrificing initial mechanical stability completely. Such initial subsidence could be interpreted as additional graft compaction and or conical wedging as tolerated with cemented polished primary implants, both effects stabilising the set-up.

The amount of initial subsidence and the logarithmically constant subsidence rate established thereafter were influenced by geometrical set-up, namely cone shape, taper angles and the dimensional ratio of cone diameter to graft mantle thickness. Alternative stem shapes and sizes altering these factors should be investigated and clinically considered for optimising impaction grafting stability. This holds particularly true for uncemented impaction grafting techniques where the surface properties are also expected to have an influence. From the good correlation between vertical and torsional stability it must be concluded that efforts to improve resistance against torsional displacement should also focus on stem shapes variations.

- **Variability of bone grafts**

Stability of morsellised pure bone grafts was not only very sensitive to procedural variables but even under supposedly constant conditions highly variable results were measured. The variability inherent in the bone graft itself could be already a major reason for the variable success rates reported for clinical impaction grafting. The high variability lies in the natural source and the complex manual graft production process. Against the relatively constant experimental conditions, in clinical application the problem is increased by variable donor health sex and age as well as different bone storage and sterilisation methods or diverse bone mill and blade types or inconsistent post-milling procedures. The impaction grafting technique using pure bone graft will remain susceptible to a variable success rate unless the inconsistencies are reduced by standardising the variable graft parameters.

From this study the following recommendations can be made. Prior to bone milling soft tissue, the large quantities of cartilage should be thoroughly removed by a scalpel. Soft tissue does not contribute to stability and even after superficial removal enough soft tissue remains available for maintaining the visco-elastoplastic properties of the morsellised graft desirable for good compaction properties. Bone graft should be morsellised with a stiff and sharp bone mill like the Howex because only such a design ensures consistent particle distribution and high operator independence. Bone graft should be washed and dried as blood, fat and other fluid phases are removed so that the delivery of impaction energy becomes more efficient by reducing the damping effect of squeezed fluids. Washing and drying can also further remove soft tissue with its low contribution to graft stability. With less soft tissue available for sealing off the porosity, cement penetration into the compacted bone graft might be enhanced and could raise stability.

Despite the low availability and high cost of human donor femoral heads surgeons should establish selection criteria based on the visual appearance and predicted mechanical quality of the heads. With one freeze and thaw cycle not significantly affecting the mechanical properties of morsellised bone graft, variability could be reduced by morsellising and mixing large quantities of femoral heads together and storing them for later use. This method would not only level out donor and preparation variability but also offers the potential to expand bone supplies by making clinical graft delivery more efficient than the preparation of discrete numbers of femoral heads. As described later, extending a morsellised allograft with a suitable ceramic also reduces variability.

- **Stability provided proximally**

Theoretical considerations about the wedging effect and experimental observations from retrieved samples after fatigue failure identified the proximal graft region to be the most load

bearing and stability providing section in the model and human femur. Thus a surgeon must pay special attention to this region during preparation of the femoral canal, graft charging and graft compaction. During post-operative loading of the implant but especially during vigorous graft impaction, the wedging effect transfers high radial stresses through the graft causing high hoop stresses in the proximal femoral wall. Bone loss, commonly associated with revision hip surgery, has often affected the quality of the proximal bone so that the risk of femoral fracture under impaction is high. Therefore, surgical measures such as wire support or even mesh reconstruction of the proximal femur are important and must be advised for impaction grafting more than for other revision techniques. Special attention should also be paid to homogenous graft mixing and charging in the proximal region to ensure homogenous load transfer and to avoid instabilities due to anisotropies. For the same reasons and for maximising stability, special attention should be given to proximal impaction quality which has to be carried out partially with handheld impactors, a process prone to inconsistencies.

- **Impaction intensity is most important**

Impaction intensity was clearly identified to be the most important single factor influencing the stability in impaction grafting and must be of prime concern for the surgeon. In particular proximal impaction with the phantom prosthesis is crucial as the wedging effect leverages the impaction effort and also introduces strong radial graft compaction. Assessment of impaction quality for maximum stability was more associated with impaction energy than impaction peak force. Increasing impaction energy improved stability more than raising the impaction forces. Too high impaction forces reduced the stability levels measured. Thus a surgeon should prioritise the delivery of high numbers of hammer blows over maximising the force of individual blows for both, distal graft pre-compaction and proximal impaction of the oversized prosthesis. Additionally, in this way the risk of femoral fracture during impaction could be reduced without sacrificing stability.

Graft stability was more sensitive to impaction energy than impaction force. This suggests that a vibratory impacting device which would operate by delivering a high number of low force blows at high frequency could produce impaction qualities and stability levels in a more consistent, user independent way. Such a tool seems a promising concept but it would be essential to ensure that peak forces of the individual hammer blows remain sufficiently high. As experimentally verified, too low impaction forces also reduce stability. Additionally, from theoretical considerations and the application of the pile driving formula one can conclude that impaction peak forces must at least exceed the peak forces occurring during the normal human gait. Otherwise, each post-operative step would act like a further impaction blow and cause corresponding levels of set per blow soon resulting in massive subsidence.

As previously mentioned, impaction quality can also be improved by washing and drying the bone graft so that impaction energy is converted into dense graft compaction and not dissipated in squeezing fluids. If impactors had a porous or grid-like surface and allowed fluid drainage which could be supported by an attached or built-in suction device, the effective delivery of impaction energy could be further enhanced. Another spring and damper effect which reduces and varies impaction energy conversion is introduced by the patient's dislocated leg which acts as the support against the hammer blows thus defining the reaction force signal and energy dissipation. Depending on leg size, weight and fixation equal impaction blows cause different peak forces and transfers efficiencies of compaction energy. If a leg moves too much during impaction, a surgeon might apply a high physical impaction effort but actually achieve less impaction than expected. Thus, stable and secure leg fixation is important and the design of positioning jig could be advantageous.

Anticipating in this context a discussion point highlighted later, adding stiff and stable ceramic granules as a bone graft extender into a bone/ceramic mix reduced the sensitivity of graft stability to impaction energies. Especially at low energy levels a high stability improvement was registered, e.g. higher stability could be achieved with less impaction effort. In a clinical context this might either reduce the risks of femoral fracture as a result of too vigorous impaction or might level out stability differences as a result of different impaction efforts by various surgeons.

Intense impaction and dense graft compaction have been advocated as the two most important factors for achieving maximum initial mechanical stability in impaction grafting. However, too intense impaction and dense graft compaction might reduce porosity and interconnectivity of void spaces or might damage trabecular bone fragments or highly porous ceramic extender granules so that revascularisation is impeded, osteoconductivity becomes reduced or cement penetration is prevented. Despite the high initial mechanical stability achieved, long term stability as a result of bone remodelling might suffer. Raising stability with less impaction energy and thus a less densely compacted graft was shown to be possible by extending bone allograft with stiff and strong ceramic bone extender granules.

- **Impaction set as stability feedback**

The complex influence of both impaction energy and impaction forces on graft stability make the intra-operative assessment or prediction of stability impossible. Impaction set depends on impaction force and accumulated impaction energy and was indeed identified as a reliable measure for predicting stability. Independent of graft materials tested, the set of the final hammer blow could be correlated with a stability level via an exponential function which was shifted for different hammer momenta. On this basis, a surgical feedback instrument could be

designed by fitting the impaction tools with a displacement transducer, which measures set per hammer blow intra-operatively. The calibration of impaction set guaranteeing stability in clinical application could be carried out by conducting impaction and stability tests with Sawbones based on the experimental procedures described in this study. As the manually delivered hammer blows cause impaction forces to vary during surgery, an average value from a few blows could be calculated as an equivalent final impaction set. Ultimately hammer forces should be controlled as well, either by intra-operative measurement or by constant delivery by a vibratory impactor as described earlier.

During testing, the exponential relationship between number of hammer blows and accumulated set was disturbed when the transducer connection came loose producing a clear shift or spike in the graph. In clinical application such monitoring could give clear and early warning of problems such as femoral cracking or displacement of the distal plug.

- **Bone plus ceramic graft mixes**

Using ceramic bone extenders in a bone/ceramic graft mix improved stability and reduced variability for most ceramic configurations and all mixing ratios tested. In a bone/ceramic mix strong ceramic granules of low friability provide additional load bearing particles of consistent properties and reduce the wetness of the graft for improved impaction efficiency. Therefore, the use of ceramic bone graft extenders can be safely recommended for clinical application to increase initial mechanical stability and produce more consistent results. Higher, more reliable initial stability would reduce cases of massive early subsidence which have been reported as an early failure mode in impaction grafting. It also encourages earlier load bearing producing the mechanical stimulus required for any osteoconductive process securing long term stability. Adding ceramic granules to bone/ceramic mix also caused the linear relationship between vertical and torsional stability to rise more steeply than with pure bone suggesting that ceramic granules increase friction between stem and graft mantle. This effect could in particular improve the stability of uncemented impaction grafting where an interlocking cement mantle is absent.

The graft stabilising effect was strongly noticed even for mixing ratios with relatively small quantities of ceramic granules. When the ceramic fraction was raised, stability improved further. The effect reduced towards high ceramic fractions but did not reverse even for the highest ceramic contents. For a surgeon this means that mixing ratios can be varied without risking any stability loss over the pure bone graft reference whether such variations are the result of mixing errors, inhomogeneous charging or deliberately adapted mixing ratios. The graft stabilising effect of ceramic bone graft extenders at any mixing ratio allows supplies of human donor allograft to be stretched and cost savings to be secured without risking negative

consequences for initial mechanical stability. In the context of ceramic graft benefits it should be reminded that the stability of b/c graft mixes is less sensitive to impaction energy levels so that bone/ceramic mixes provide stability superior to pure allograft at lower impaction energy levels. Therefore, extending morsellised allograft with ceramic granules clinically promises to reduce the effects of different surgical impaction efforts on stability. Equal stability at lower impaction energies for b/c mixes might also help to reduce the risk of femoral fracture during impaction or to maintain a structurally intact graft with interconnected porosity.

Despite the superior overall stability of bone/ceramic mixes over pure allograft, the b/c mixes showed some initially higher subsidence and at lower loads than the densely compacted allografts. The superior overall stability of the mixes was the result of significantly less steeply increasing subsidence rates than those of pure allograft which more resembled a massive collapse once a certain peak force was exceeded. The clinical advantage of using bone/ceramic mixes is that even if some initial subsidence occurs post-operatively, the graft mixes promise to stabilise on a new plateau while initial subsidence with pure allografts can be the precursor of a near graft collapse. There is hope that early subsidence with bone/ceramic mixes stabilises below displacement levels requiring re-revision while with pure allografts under these circumstances re-revision seems more likely.

Configurations of ceramic graft extender

Varying the configurations of the ceramic phase in the bone/ceramic graft mixes singled out porosity as the most critical parameter. Increasing porosity levels, pore size, and pore interconnectivity is biologically desirable for optimal osteoconductive properties of the synthetic extender. However, too high porosity combined with the inherent brittleness of a ceramic can result in dramatically reduced mechanical stability and high friability. During testing low porosity levels hardly affected the performance over a non-porous reference, but at the maximum porosity level the bone/ceramic mix was mechanically weaker than even a pure allograft. Such highly porous ceramics must not be recommended for clinical application. The biological advantages promised by such a highly porous ceramic will be virtually destroyed during impaction which can deliver higher peak forces into the graft than the fatigue loading process. Defining an optimum porosity level for a ceramic bone graft extender demands a conservative compromise between mechanical and biological requirements be found.

Sintering of the ceramic granules must be completed at sufficiently high temperatures and times to secure highest stability. Lowering the sintering temperature, possibly in order to manipulate graft resorption rates or osteoconductivity, can result in dramatically increased friability and reduced stability when sintering was incomplete. If resorption rates are supposed

to be manipulated than it should be done by the chemical composition ratio between HA and TCP. Here the influence on the mechanical stability of a bone/ceramic mix seemed negligible.

With regard to the particle size of the ceramic phase in the bone/ceramic graft mixes, a medium 2-4mm particle size was found to deliver superior stability over small and large particles. The medium particle size balances the graft subsidence mechanisms of fracture and re-arrangement for maximum stability and leads to optimal mixing and charging with bone graft. Clearly, the optimum particle size depends on the size of the cavity impacted into and therefore large particles are recommended on the acetabular side where the void space is significantly larger than on the femoral side. Graft mixing, charging and packing could theoretically be improved further with a ceramic size mix. However, the small cavity gaps between stem and endosteal wall make it impossible for a graft mix with increased phase complexity to ensure homogenous mixing and charging.

Graft stability in impaction grafting is the result of complex phase interactions between strong load bearing phases such as trabecular bone chips or ceramic granules and less strong, viscoelastic soft tissue required for compaction and graft cohesion plus the fluid phases such as blood influencing impaction effectiveness. It can be concluded that only such a phase mix can provide optimum stability in impaction grafting which can be increased by raising the content of reproducibly strong ceramic extenders. If it is the goal to replace bone graft in impaction grafting entirely by some synthetic material such a material must also offer a combination of strong, load bearing properties and viscoelastic, compactable properties. Thus it must be a mix as well or a composite material such as a ceramic reinforced resorbable polymer.

Facing the conflict between maximum initial mechanical stability and long term stability as the result of graft revascularisation, graft incorporation, bone deposition, graft resorption and remodelling, initial mechanical stability should be given the priority. Preventing subsidence and providing stiffness to limit micromotion, initial stability is the prerequisite for any secondary osteoconductive effects. The time-dependent functions of degrading initial mechanical stability and increasing long-term stability as a result of graft resorption and bone remodelling are unknown. No predictions can be made as to whether total stability remains constant or even drops temporarily during these processes or if resorption and remodelling rates can be manipulated to maintain high total stability. When a synthetic material is to be selected for clinical use as a bone graft extender it should be selected on the basis of providing high initial mechanical stability as opposed to rapid osteoconductive activity. A slowly or even partially non-resorbed graft which provides high initial mechanical stability has the potential to provide long term stability as well.